K-SHELL IONIZATION CROSS SECTIONS OF SELECTED ELEMENTS FROM FE TO AS FOR PROTON BOMBARDMENT FROM 0.5 TO 2.0 MEV

DISSERTATION

Presented to the Graduate Council of the
North Texas State University in Partial
Fulfillment of the Requirements

For the Degree of

DOCTOR OF PHILOSOPHY

By

Richard D. Lear, M.S.
Denton, Texas

December, 1973

Lear, Richard D., K-Shell Ionization Cross Sections of Selected Elements from Fe to As for Proton Bombardment from 0.5 to 2.0 MeV. Doctor of Philosophy (Physics), December, 1973, 65 pp., 3 tables, 8 illustrations, bibliography, 47 titles.

The problem with which this investigation is concerned is that of making experimental measurements of proton-induced K-shell x-ray production cross sections and to study the dependence of these cross sections upon the energy of the incident proton. The measurements were made by detection of the characteristic x-rays emitted as a consequence of the ionization of the K-shell of the atom. The method for relating this characteristic x-ray emission to the x-ray production cross section is discussed in this work.

The measurements made in this investigation have a two-fold use. First, they add to needed information for testing of theoretical calculations of inner atomic electron shell ionization by ion impact. There are three basic theories which describe inner shell ionization processes. Two of these theories, the Binary Encounter Approximation (BEA) and the Plane Wave Born Approximation (PWBA), apply to the proton energy range studied in this work. The BEA is a semi-classical treatment, and the PWBA is a quantum mechanical treatment. Corrections have been suggested to the PWBA to account for the change in the binding energy of the ionized shell caused

by the penetration of the incident ion into this shell. This gives three theoretical predictions applicable to this work.

Two of the theories, the BEA and the PWBA with binding energy corrections, give nearly equivalent predictions for the ionization cross section of an element when bombarded by protons in the energy range investigated in this work. The PWBA predicts cross sections which may differ from the other predictions by as much as a factor of two. Because of insufficient data to totally test these three theories, it is not known which theory best predicts the ionization cross sections for the range of proton energies studied in this work. The measurements made here compliment existing data and aid in the testing of these theories.

The second use of these measurements is in the field of application of x-ray analysis. High resolution non-dispersive x-ray detectors have made x-ray techniques important as a non-destructive analytical tool. X-ray analysis techniques have been found useful for such work as pollution analysis and characterization of solid-state samples. Studies are also being done which apply x-ray analysis techniques to medical research. The most promising method of x-ray excitation is by ion bombardment. Large cross sections for x-ray production and lower intensity bremsstrahlung radiation in comparison to electron bombardment make this a most sensitive means for detection of trace amounts of elements. To increase the utility of this method for quantitative analysis, values for x-ray

production cross sections are needed. Since the available data is limited, the measurements of this work are a useful contribution to the information needed for studies in x-ray analysis techniques.

The K-shell ionization and x-ray production cross sections for Fe, Co, Cu, Zn, Ga, Ge, and As were measured for proton impact in the range 0.5 to 2.0 MeV. Several of these elements were chosen for this investigation because of the need for x-ray production cross sections to facilitate the characterization of materials used in semi-conductor devices. The ionization cross sections for Fe, Co, Cu, Zn, Ga, Ge, and As were found to be 242±23, 173±15, 94.1±7,8, 70.9±6.9, 56.4±4.6, 36.5±2.7 and 27.1±2.1 barns respectively at 2.0 MeV. These measurements agree to within less than 17 per cent with the predictions of the BEA and the PWBA with binding energy corrections. The predictions of the PWBA exceed the measured values by as much as a factor of two at the maximum deviation. It is concluded from a study of the energy dependence of these cross sections that the BEA and PWBA with binding energy corrections continue to give a superior prediction to the PWBA over the proton energy range 0.5 to 2.0 MeV. These measurements also indicate a trend for the measured ionization cross sections to drop below the predictions for all three theories for low projectile energies as well as an increasing disagreement between the measurements and the predictions of the BEA and corrected PWBA as the atomic number of the target decreases.

TABLE OF CONTENTS

LIST OF TABLES

LIST OF ILLUSTRATIONS

CHAPTER I

INTRODUCTION

The study of characteristic x-rays has been active for many years. Characteristic x-rays were first observed and identified by Chadwick[1] in 1912. The x-rays were produced by the exposure of thick targets of several elements to alpha particles from radium. K-shell x-rays from Z = 32 to 79, L-shell x-rays from Z = 34 to 79, M-shell x-rays for Z = 83 were excited and measured by Bothe and Franz[2] in 1928 by bombardment with alpha particles from polonium.

In 1930 Barton[3] unsuccessfully attempted to produce x-rays by bombardment of materials with low energy protons. Grethsen and Reusse[4] successfully preformed this experiment in 1933 with 30 to 150 keV protons. Livingston, Genevese and Konopinski[5] in 1937 studied characteristic x-rays from targets in the range Z = 12 to 82 produced by proton bombardment up to 1.76 MeV. These data as well as that of Grethsen and Reusse[4] agreed with theoretical predictions by Henneberg[6] made in 1933.

In 1953 Lewis *et al.*,[7] using NaI detectors, studied K-shell x-rays from thick targets of Mo, Ta, Au, and Pb produced by proton bombardment in the range 1.7 to 3.0 MeV.

Lewis and Bernstein[8] studied L-shell x-rays from thick targets of Ta, Au, Pb, and U produced by proton impact in the range 1.5 to 4.25 MeV.

Hansteen and Messelt,[9] in 1956, used NaI detectors to measure x-ray production cross sections for proton impact in the range 0.2 to 1.6 MeV on Cu and Mo foils. In 1957, Singh[10] used proportional counters to study K-shell x-rays from Cu and Ag foils produced by impact of protons, deuterons and alpha particles. Also in 1957, Messelt[11] reported K-shell x-ray production cross sections for thick targets of Fe, Cu, Mo, Ag, Sn, and Ta by proton bombardment in the range 0.14 to 1.3 MeV.

From 1962 to 1967 Jopsen et al.[12] and Khan et al.[13-20] did considerable work on x-ray production and ionization cross section measurements by low energy proton impact. They used scintillation and proportional counters to measure K, L, and M-shell radiations from thick targets.

In 1969 Hart et al.[21] used gas proportional counters to measure cross sections for K-shell x-ray production in thin layers of Al_2O_3 by bombardment with 0.02 to 0.1 MeV protons.

Studies of characteristic x-rays have recently received renewed interest because of the availability of high resolution non-dispersive Si(Li) x-ray spectrometers. In 1966, E. Elab and M. Nakamura[22] first reported development of non-dispersive Si(Li) detectors for photon detection. They reported detection of Fe K-shell x-rays from the decay of ^{57}Co

and Ag L-shell x-rays from the decay of ^{109}Cd. Since this work several investigators have employed commercially available Si(Li) detectors for x-ray studies.

These new measurements have renewed an interest in the study of the theory for calculating charged particle ionization cross sections. Theoretical investigations of inner atomic electron shell ionizations by ion impact have been developed semi-classically in the Binary Encounter Approximation (BEA) by Garcia, Gerjouy, and Welker,[23] quantum mechanically in the Plane Wave Born Approximation (PWBA) by Khandelwal, Choi and Merzbacher[24] and in an impact parameter method by Bang and Hansteen.[25] The latter theory applies to the case where the energy of the incident particle is near the binding energy for the electron removed. The projectile energies used in these experiments are well above the threshold energy and in the range where the first two theories apply. Both of these theories assume the primary interaction between the incident ion and the orbital electron is coulombic. These two theories will be discussed in more detail in Chapter II.

Since the development of these high resolution x-ray detectors, x-ray techniques have also become important as a non-destructive analytical tool. The most promising method of x-ray excitation is by ion bombardment. Large cross sections for x-ray production and lower intensity bremsstrahlung radiation in comparison to electron bombardment

make this a most sensitive means for detection of trace amounts of elements.[26,27] To increase the utility of this method for quantitative analysis, values for x-ray production cross sections are needed. However, values are available only for selected elements over a limited energy range.[28]

Although several authors have reported measurements of x-ray processes for protons on thick targets from Fe to As at selected proton energies below 2000 keV,[4, 11-14, 20, 29] further study is needed in this energy range because of problems associated with thick target yields. The reduction of thick target x-ray data to give the x-ray production cross section involves the measurement of the slope of the thick target excitation function and the use of stopping powers for the incident ions. Uncertainties in these quantities have led to results whose errors are typically of order 30 per cent or higher. Predictions by the above mentioned theories are not suitable for analytical work because of disagreement between the theories and a lack of data to test the predictions of each. This disagreement will be discussed in more detail in the next chapter.

The work reported here was undertaken to provide ionization cross sections for comparison to the theories and for use in quantitative measurements.

CHAPTER II

THEORY

As stated in the introduction, there are two basic theories applicable to this energy range for calculating the ionization cross section for ion impact. The impulse approximation considers the dominant interaction producing the ionization to be a direct energy exchange between the incident charged particle and the bound electron. Calculation of the cross section ($\sigma_{\Delta E}$) for exchange of an amount of energy ΔE between two moving charged particles was done by Gerjuoy.[30] Garcia, Gerjuoy and Welker[23] developed a theory of ionization by proton impact based on the work by Gerjuoy. This theory assumes the only effect of the nucleus of the target atom is to establish the momentum distribution of the electrons. The collision, via a coulomb interaction only, is assumed to be between two free charged particles. Thus the name Binary Encounter Approximation (BEA) is used.

In developing the BEA Garcia, et al. first consider a collision between two free charged particles 1 and 2 moving with velocities $\vec{v}_1 = v_1\vec{n}_1$ and $\vec{v}_2 = v_2\vec{n}_2$ in the laboratory frame. After collision their laboratory velocities will be $\vec{v}_1' = v_1'\vec{n}_1'$ and $\vec{v}_2' = v_2'\vec{n}_2'$. Throughout this development

a bar below the symbol will denote a center of mass variable and a prime will denote a post-collision variable. The relative velocity between the two particles will be denoted before and after the collision respectively by $\vec{v} = \vec{v}_1 - \vec{v}_2 = v\vec{n}$ and $\vec{v}' = \vec{v}_1' - \vec{v}_2' = v'\vec{n}'$. The center of mass velocity is given by

$$\vec{V}_{CM} = V_{CM}\vec{n}_V = M^{-1}(m_1\vec{v}_1 + m_2\vec{v}_2)$$

where $M = m_1 + m_2$. The relationship between the laboratory and the center of mass velocities is given by the usual relationship of $\vec{v}_i = \vec{V}_{CM} + \vec{\underline{v}}_i$. From this relationship it follows that $\vec{v} = \vec{v}_1 - \vec{v}_2 = \vec{\underline{v}}_1 - \vec{\underline{v}}_2 = v\vec{\underline{n}}$. The same relations hold after collision.

By choosing the polar axis of a fixed system along $\vec{V}_{CM}$ the polar and azimuth angles of $\vec{\underline{n}}$ and $\vec{\underline{n}}'$ are $\underline{\theta}$, $\underline{\phi}$ and $\underline{\theta}'$, $\underline{\phi}'$ respectively as shown in Figure 1.

Let particle 1 be the incident projectile. The energy gained (ΔE) by particle 2 (as seen in the laboratory system) can be shown to be:[30]

$$\Delta E = \mu v V_{CM}(\cos\underline{\theta} - \cos\underline{\theta}')$$

where $\mu = m_1 m_2 M^{-1}$ is the reduced mass. Thus for a given $\vec{v}_1$ and $\vec{v}_2$ the energy transferred (ΔE) is a function of $\underline{\theta}'$. Differentiating the energy transfer equation gives

$$d(\Delta E) = \mu v V_{CM}(\sin\underline{\theta}' d\underline{\theta}').$$

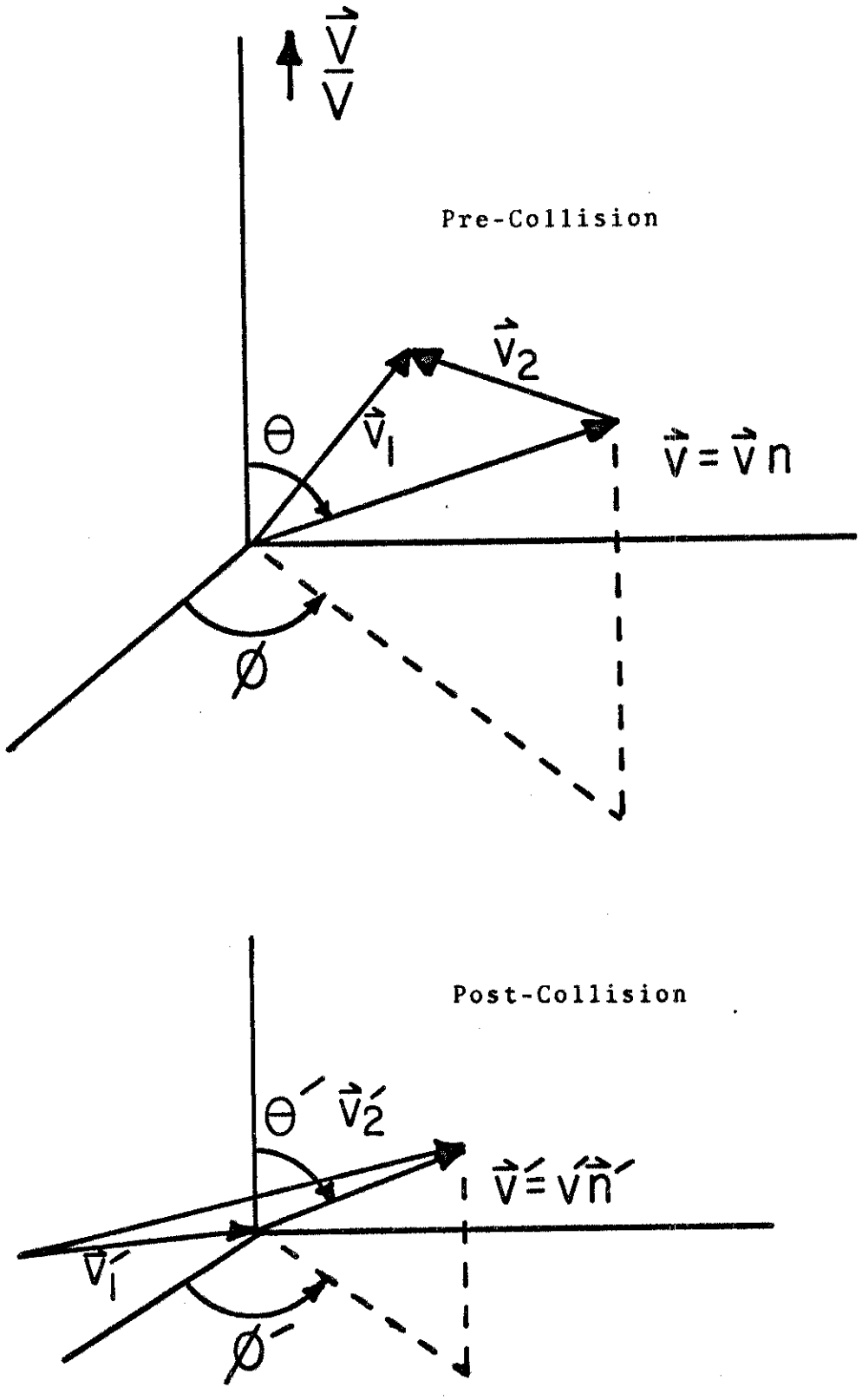

Fig. 1--Coordinate System for BEA

The total cross section for transfer of all possible amounts of energy is given by

$$\sigma(\vec{v}_1,\vec{v}_2) = \int \sigma_{\Delta E}(\vec{v}_1,\vec{v}_2)\, d(\Delta E).$$

If $\underline{\sigma}(v;\vec{\underline{n}}\rightarrow\vec{\underline{n}}')$ is the corresponding differential scattering cross section in the center of mass system[30], then

$$\sigma(\vec{v}_1,\vec{v}_2) = \frac{1}{\mu v V_{CM}} \int d(\Delta E)\, d\underline{\phi}'\, \underline{\sigma}(v;\vec{\underline{n}}\rightarrow\vec{\underline{n}}').$$

The last two equations imply

$$\sigma_{\Delta E}(\vec{v}_1,\vec{v}_2) = \frac{1}{\mu v V_{CM}} \int d\underline{\phi}'\, \underline{\sigma}(v;\vec{\underline{n}}\rightarrow\vec{\underline{n}}').$$

The prominent interaction is assumed to be coulombic. This assumption designates $\underline{\sigma}$ as the Rutherford cross section i.e.,

$$\underline{\sigma}(v;\vec{\underline{n}}\rightarrow\vec{\underline{n}}') = \left(\frac{Z_1 Z_2 e^2}{2\mu v^2}\right)^2 \csc^4(\chi/2)$$

where χ is the scattering angle between $\vec{\underline{n}}$ and $\vec{\underline{n}}'$ in the center of mass system and $Z_1 e$, $Z_2 e$ are the charges of the interacting particles. The relationship between the scattering angle and the angles which locate the relative velocity vectors is given by

$$\cos\chi = \cos\underline{\theta}\cos\underline{\theta}' + \sin\underline{\theta}\sin\underline{\theta}'\cos(\underline{\phi} - \underline{\phi}').$$

Using the above relationship and the expression for the differential Rutherford cross section, it follows that[30]

$$\sigma_{\Delta E}(\vec{v}_1,\vec{v}_2) = \frac{2\pi(Z_1 Z_2 e^2)^2 V_{CM}^{\ 2}}{v^2 |\Delta E|^3}\left(1 - \cos^2\underline{\theta} - \frac{\Delta E}{\mu v V_{CM}}\cos\underline{\theta}\right)$$

where

$$-1 \leq \cos\underline{\theta} - \frac{\Delta E}{\mu v V_{CM}} \leq 1,$$

otherwise $\sigma_{\Delta E} = 0$. This restriction guarantees that $\sigma_{\Delta E} \geq 0$.

The above expression for $\sigma_{\Delta E}$ is a function of the velocities of the two colliding particles. The quantity needed for the calculations of the ionization cross sections is the effective average of $\sigma_{\Delta E}(\vec{v}_1, \vec{v}_2)$ over all orientations of $\vec{v}_1$ and $\vec{v}_2$ for fixed speeds v_1, v_2, i.e., $\sigma_{\Delta E}^{eff}(v_1, v_2)$.

If particle 2 has an isotropic velocity distribution in the laboratory system then the effective $\sigma_{\Delta E}$ is defined by[23]

$$v_1 \sigma_{\Delta E}^{eff} = \frac{1}{4\pi} \int d^3 n_2 \, |\vec{v}_1 - v_2 \vec{n}_2| \, \sigma_{\Delta E}(\vec{v}_1, \vec{v}_2).$$

This definition applies to the case where particles 2 are electrons bound to a stationary atom being ionized by a beam of incident protons. In the case of an isotropic distribution for $\vec{v}_2$, $\sigma_{\Delta E}^{eff}$ cannot depend upon the direction of $\vec{n}_1$. Thus $\sigma_{\Delta E}^{eff}$ depends upon the magnitude of $\vec{v}_1$ and $\vec{v}_2$ and can be averaged over $\vec{n}_1$ as well as $\vec{n}_2$.

Garcia *et al.*[23] show that the ionization cross section for proton impact is given by

$$\sigma_{ion} = \sum_i n_i \int_{U_i}^{E_1} \sigma_{\Delta E}^{eff}(v_1, v_2; \lambda) \, d(\Delta E)$$

where λ is the ratio of the proton mass to electron mass, n_i is the number of electrons having ionization energy U_i

and E_1 is the incident proton energy. The resultant cross section must then be averaged over the speed distributions of the orbital electrons. Garcia et al. have done the indicated integrations and the results are listed on page 67 of reference 23.

The speed distribution of the bound electrons can be determined classically from a microcanonical ensemble from the expression

$$f(v_2) = c \int \delta(H - E_1) d^3r$$

where $H = mv_2^2/2 + Ze^2/r$. Garcia[31] has shown for a hydrogenic atom with an electron in a total energy state $(-U)$, that

$$f(v_2) = \frac{32}{\pi} v_o^5 \left(v_2^2/(v_2^2 + v_o^2)^4 \right)$$

where $v_o = (2U/m)^{\frac{1}{2}}$.

Garcia, Fortner and Kavanagh[32] have done the averaging of σ_{ion} over the above velocity distribution function by numerical techniques and published the results in tabular form for the case of proton ionization of the K-shell. It was this table which was used in generating the BEA predictions used in this work. Appendix A gives an example of calculations from this table.

The second theory which applies to the experiments discussed in this work is the quantum mechanical treatment originating from the Born Approximation. The Born Approximation gives the differential scattering cross section as

$$\frac{d\sigma}{d\Omega} = \frac{M^2}{4\pi^2\hbar^4}\left|\left\langle \Psi_f | V | \Psi_I \right\rangle\right|^2$$

where M is the reduced mass of the particle incident upon the atom. Since the interaction is assumed to be totally Coulombic, the interaction potential is taken as

$$V = \frac{Ze^2}{|\vec{R} - \vec{r}|}$$

where Ze is the charge of the incident particle, $\vec{R}$ is the position vector pointing from the atom to the particle and $\vec{r}$ denotes the position of the atomic electron relative to the nucleus. Thus $|\vec{R} - \vec{r}|$ is the separation distance between the incident particle and the ejected electron. Figure 2 shows this coordinate system. The initial and final wavefunctions are taken to be[33]

$$\Psi_I = \Psi_n \exp(i\vec{P}\cdot\vec{R}/\hbar)$$

and

$$\Psi_F = \Psi_{n'} \exp(i\vec{P}'\cdot\vec{R}/\hbar)$$

respectively, where Ψ_n and $\Psi_{n'}$ are the initial and final wavefunctions of the electron, $\vec{P}$ and $\vec{P}'$ are the initial and final momenta of the incident particle and the exponential functions are the plane wave representations of the incident particle. Making the indicated substitutions yields the following relationship for the differential scattering cross section

$$\frac{d\sigma}{d\Omega} = \frac{M}{4\pi^2\hbar^4}\frac{v'}{v}\left|\int \Psi^*_{n'}(\vec{r})\frac{Ze^2\exp(i\{\vec{P} - \vec{P}'\}\cdot\vec{R}/\hbar)}{|\vec{R} - \vec{r}|}\Psi_n(\vec{r})\,d\vec{r}d\vec{R}\right|^2$$

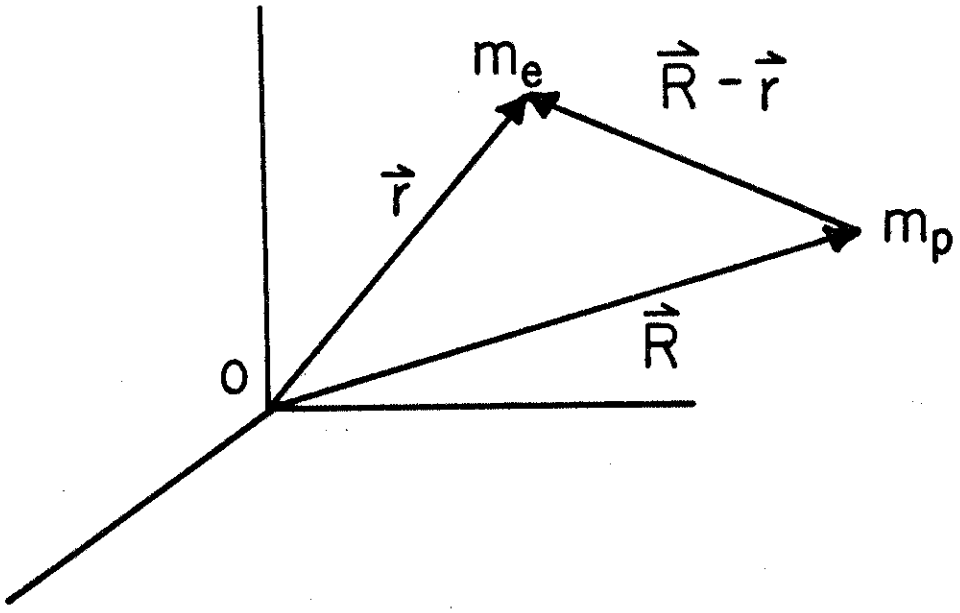

Fig. 2--Coordinate System for PWBA

where v and v′ are the initial and final speeds of the electron.

Merzbacher and Lewis[33] state that by making the substitution $\hbar\vec{q} = \vec{P} - \vec{P}'$ and integrating over the coordinates of the particle the above expression yields

$$d\sigma = 8\pi Z^2 \left(\frac{e^2}{\hbar v}\right)^2 \frac{dq}{q^3} \left| \int \psi_{n'}^{*}(\vec{r}) \exp(i\vec{q}\cdot\vec{r})\, \psi_n(\vec{r})\, d\vec{r} \right|^2 .$$

The form factor is defined as

$$F_{n'n}(q) = \int \psi_{n'}^{*} \exp(i\vec{q}\cdot\vec{r})\, \psi_n\, d\vec{r} .$$

Summing the above expression for the differential cross section over all the substates of an initially filled atomic shell (labelled s) and integrating over all directions of the ejected electron, Merzbacher and Lewis[33] show the differential cross section for transfer of energy between ε and $\varepsilon + d\varepsilon$ becomes

$$d^2\sigma_{\varepsilon s} = 8\pi Z^2 \left(\frac{e^2}{\hbar v}\right)^2 \frac{2dq}{q^3} \left| F_{\varepsilon s}(q) \right|^2 d\varepsilon$$

where ε is the amount of energy transferred to the atom. The factor 2 enters because of the double occupancy of each inner electron orbit. Now the dimensionless quantities $w = \varepsilon/(Z_s^2 R_\infty)$ and $Q = a_s^2 q^2$ are introduced where R_∞ is Rydberg's constant, Z_s is the effective nuclear charge for the s shell,[24] and $a_s = a_o/Z_s$, a_o being the Bohr radius of hydrogen. The effective nuclear charge Z_s takes into account the screening of the s shell by an inner shell or subshell. The values of

Z_s used to develope the PWBA were determined by Slater[39] from interpretation of optical data. Making the above substitutions gives the cross section for ionization of the s shell as

$$\sigma_s = 8\pi^2 Z^2 \left(\frac{e^2}{h\nu}\right)^2 \frac{a_o^2}{Z_s^2} \int_{w_{min}}^{w_{max}} dw \int_{Q_{min}}^{Q_{max}} \frac{dQ}{Q^2} \left| F_{ws}(Q) \right|^2 .$$

If the energy loss is small as compared to the laboratory energy of the incident particle the lower limit of Q is given by

$$Q_{min} = w^2/4\eta_s$$

where

$$\eta_s = \frac{1}{Z_s^2} \left(\frac{h\nu}{e^2}\right)^2 = \frac{m_e}{m_p Z_s^2} \frac{E}{R_\infty}$$

for protons. Under the same conditions the upper limit of Q is given to a very good approximation by $Q_{max} = \infty$.

The amount of energy transferred ($wZ_s^2R_\infty$) is related to the kinetic energy of the emitted electron (T) by

$$wZ_s^2R_\infty = T + U_s$$

where U_s is the ionization potential of the s subshell. This relationship implies that the minimum value of w is given by

$$w_{min} = U_s/(Z_s^2R_\infty)$$

when T = 0. The maximum value of w is approximated by $w_{max} = \infty$.

Khandelwal, Choi and Merzbacher[24] define an "ideal ionization potential" (θ_s) by

$$\theta_s = U_s s^2/(Z_s^2 R_\infty)$$

where s is a screening number indicative of the shell being ionized, i. e. s = 1 for K-shell, s = 2 for L-shell. So for the K-shell θ_s is equivalent to w_{min}. Introduction of these limits to the integrals gives the K-shell ionization cross section as

$$\sigma_K = 8\pi \left(\frac{e^2}{hv}\right)^2 \frac{a_o^2}{Z_K^2} \int_{\theta_K}^{\infty} dw \int_{w^2/4\eta_K}^{\infty} \frac{dQ}{Q^2} \left| F_{wK}(Q) \right|^2 .$$

Making the definition

$$f_K = \int_{\theta_K}^{\infty} dw \int_{w^2/4\eta_K}^{\infty} \frac{dQ}{Q^2} \left| F_{wK}(Q) \right|^2$$

and using the definition of η_s allows the ionization cross section to be written as

$$\sigma_K = \frac{8\pi a_o^2}{Z_K^4 \eta_K} f_K .$$

Khandelwal *et al.*[24] have published a set of tables which give values of f_K as a function of θ_K and η_K. These tables have been used in this work to calculate the Plane Wave Born Approximation (PWBA) predictions of the ionization cross sections. Appendix B gives an example of calculations from these tables.

The tables available for each theory must be interpolated to calculate ionization cross section values at even

intervals which would be convenient to operate at in the laboratory. The computer code (for the IBM 360/50 system) SIGCAL was written to do these interpolations. The code then calculates the cross section as a function of energy. Because of the restrictive nature of the tables themselves, the code was written only for K-shell ionization by proton impact. The requirements of this work necessitated an energy range only from 0.3 to 3.0 MeV. Appendix D gives a listing of this program and a typical set of results.

These two theories, the BEA and the PWBA, differ by as much as a factor of two over the range of these experiments. The PWBA consistently gives a prediction larger than the BEA. The data that is available indicates that the BEA is in best agreement with the experimental measurements.

Basbas, Brandt and Lubert[35] have reported a correction to the PWBA to account for the change in ionization energy of the atom caused by the penetration of the incident particle into the shell being ionized. This correction becomes increasingly more important as the energy of the incident particle decreases. The impact parameter necessary to cause significant ionization becomes small enough that the time the incident particle remains in the shell which it ionizes is large compared to the response time required for the electrons to adjust to the presence of the particle. This has the effect of increasing the binding energy and reducing the probability of ionization.[36,37] Basbas *et al.*

have shown that the relationship between the original binding energy and the perturbed binding energy is given by

$$U' = \varepsilon U$$

where

$$\varepsilon = 1 + \frac{2Z_1}{Z_K\theta_K} g_K(\xi_K)$$

and $g_K(\xi_K)$ is given to within one per cent by

$$g_K(\xi_K) = (1 + \xi_K)^{-5} \left(1 + 5\xi_K + 7.14\xi_K^2 + 4.27\xi_K^3 + 0.947\xi_K^4\right)$$

with

$$\xi_K = \frac{2(\eta_K)^{1/2}}{\theta_K} .$$

Mott[38] has shown that the calculations proceed the same except the original binding energy is replaced with the perturbed binding energy. In the PWBA this amounts to replacing θ_K with $\varepsilon\theta_K$. These calculations, termed the corrected PWBA, were made for comparison with the other theories and the measurements made in this experiment. The comparison to the data will be discussed later. Appendix C gives a sample calculation of the perturbed binding energy and its result on the ionization cross section.

These corrections, as suggested by Brandt[37] were incorporated into the computer code SIGCAL. The code does both the corrected and uncorrected PWBA calculations as well as the BEA calculations. The corrected form of the PWBA is included in the program listed in Appendix D.

CHAPTER III

EXPERIMENTAL PROCEDURE

Figure 3 shows the experimental station. Targets were placed in the vacuum system at a 45 degree angle to the beam. Proton beams of up to 200 nanoamperes from an HVEC 2MV Van de Graaff were incident on the target. The incident proton beam was energy analyzed to an energy of $E_p \pm 2.0$ keV by use of a calibrated magnet system. The magnetic field was monitored by a Hall probe. The 1.85 MeV threshold of the $^{7}Li(p,n)^{7}Be$ reaction was used to calibrate the system. The projectile energy was then calculated from the expression

$$E = C(HPV)^{2}$$

where C is a constant determined in the calibration and HPV is the Hall probe voltage. Beam current integration was accomplished by standard techniques.

A KEVEX Si(Li) x-ray detector with a resolution of 172 ev at 5.9 keV was placed outside the vacuum system at 90 degrees to the beam. The x-rays produced in the target were brought out of the vacuum system through a 0.0125 mm mylar window. These x-rays were then passed through a 0.025 mm Be window on the detector cryostat and entered the 30 mm^2 x 3mm active detector volume. The detector was used

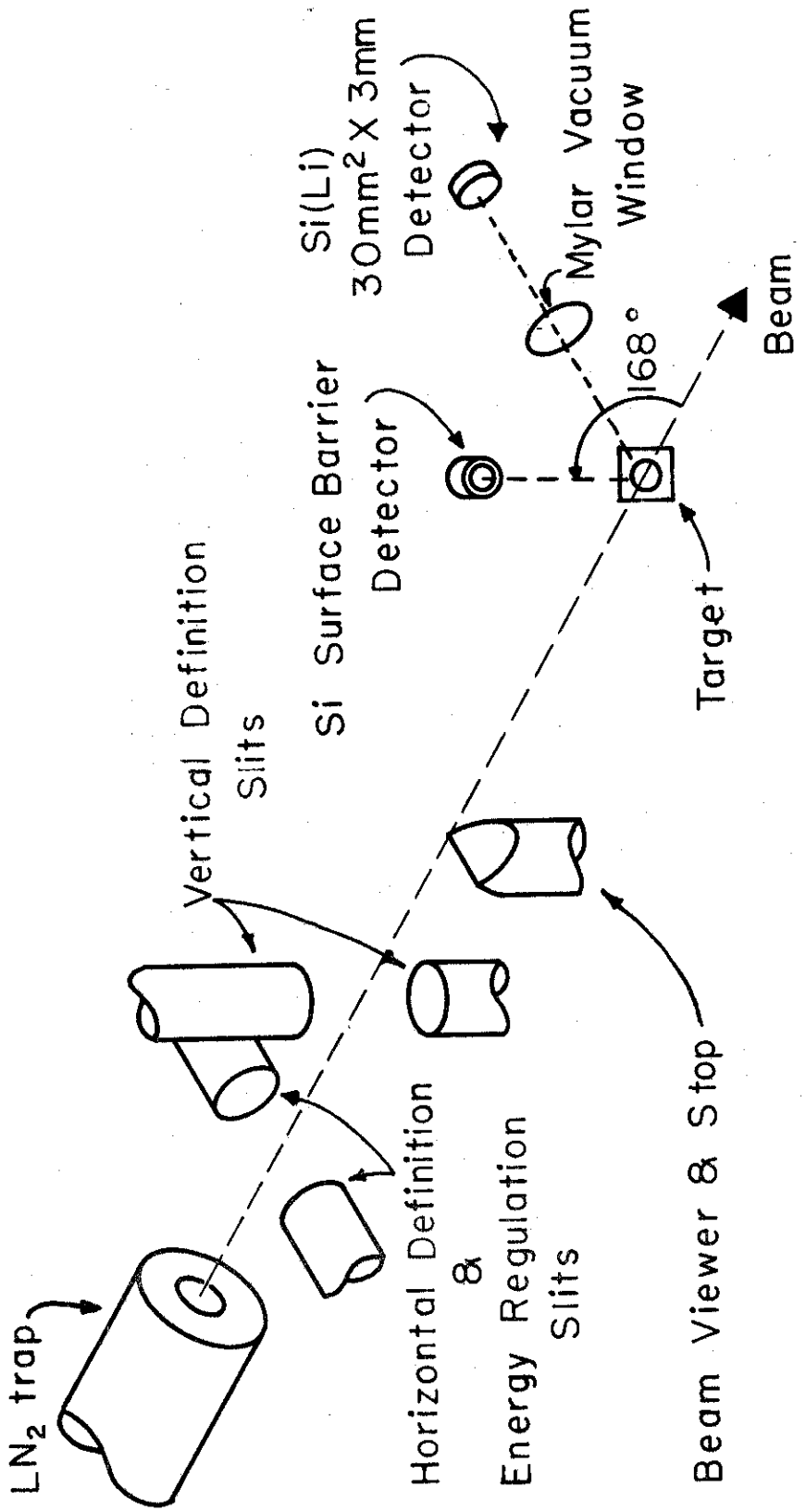

Fig. 3--Experimental Station

in conjunction with a standard electronics support package consisting of a preamplifier, amplifier, bias supply, pulse pile-up rejector, and dead time corrector. This electronics package was interconnected with the beam current integrator and multi-channel analyzer so dead time corrections were made electronically. Figure 4 shows a block diagram of the electronics.

A 340μ silicon surface barrier detector, used to measure target thicknesses by standard backscattering techniques, was placed internal to the vacuum system at an angle of 168 deg. to the beam direction. A 1.5 mm diameter collimator was placed in front of this detector to restrict the counting area to the central portion of the detector. The solid angle subtended by the detector with respect to the beam spot was measured using a standardized ^{244}Cm alpha emitting source. The alpha source was placed in the target position and the solid angle determined from the number of alpha particles (N_α) detected during time T by the expression

$$\Omega = 4\pi N_\alpha / (TI)$$

where I is the intensity of the ^{244}Cm source in alpha particles per second. The solid angle was found to be 1.53×10^{-4} sr. by this method. The solid angle was also calculated from measurements of the detector-target geometry. The assumption was made that the detector face was normal to a line from the center of the target to the center of the detector. A point source geometry was also assumed for ease

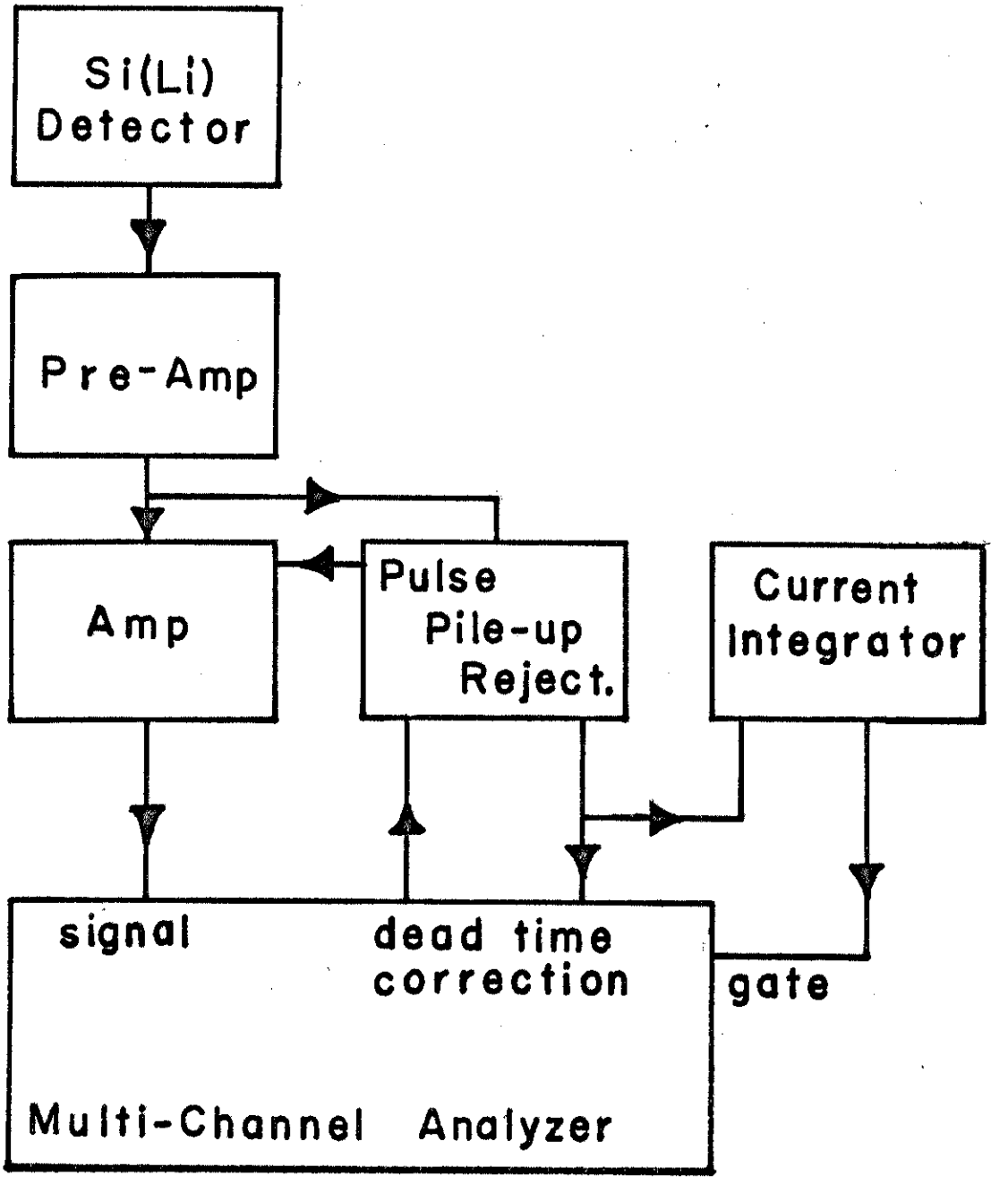

Fig. 4--Block Diagram of Electronics

of calculation. This calculation gave the solid angle as 1.95×10^{-4} sr. The difference between the measured value and the calculated value is attributable to the assumptions made in the calculations.

A study of the effects of variation of beam spot size on solid angle revealed no corrections were necessary to account for the difference between the beam spot and the alpha source. The beam definition slits, as shown in Figure 3, were opened to double the area of the beam spot with no detectable difference in the solid angle.

The absolute detector-system efficiency of the x-ray detection system was determined experimentally using x-rays from standardized sources as described in the literature by Gehrke and Lokken[39]. The absolute efficiency includes the solid angle, absorption of x-rays in the air and detector windows and efficiency characteristics of the Si(Li) crystal. The efficiency measurements were made by placing an x-ray emitting source in the target position and recording the number of x-rays (N_x) detected during an amount of time T. The efficiency is then calculated from the relationship

$$\varepsilon = N_x/(I_x T)$$

where I_x is the x-ray intensity of the source. Gehrke *et al.*[39] and Hansen *et al.*[40] have developed tables which relate x-ray intensities of a source to its γ-ray intensity. The energy dependence of the efficiency was determined by using several standardized sources which emit a spectrum of low energy

x-rays and γ-rays. Table I lists the sources used and their corresponding photon energies. Figure 5 is a plot of the efficiency vs energy curve determined in this experiment. The solid line is a least squares fourth order polynomial fit to the data.

Foil targets mounted to transmit the beam were fabricated from Fe, Co, Cu, Zn, Ge, and As for use in this work. Self-supporting carbon backings were first affixed to aluminum target frames. The element to be investigated was then deposited on the backing by standard vacuum evaporation techniques. Table II lists the target thicknesses used in this work.

The only element investigated which was not prepared by this technique was Ga. Other techniques had to be used because the melting point of Ga is 29.78° C. An 800 Å gallium-nitride film grown epitaxially on a Si substrate was obtained from Texas Instruments, Inc. for use in this work. No target degradation was apparent during experiments on this sample. An elevated count rate in the x-ray detector was encountered with this sample due to the characteristic x-rays from Si and the proton induced bremsstrahlung in the substrate. Addition of a 2 mil mylar absorber between the target and the detector attenuated this low energy radiation and lowered the count rate to a level compatable with the analyzing electronics. Corrections were made for the additional attenuation of the characteristic Ga radiations by this absorber.

TABLE I

EFFICIENCY CALIBRATION SOURCES

Source	Photon Energy (keV)
^{51}Cr	5.0
^{54}Mn	5.47
^{57}Co	6.46
	14.36
^{65}Zn	8.2
^{241}Am	11.9
	13.9
	17.8
	20.8
	26.4
^{137}Cs	32.1

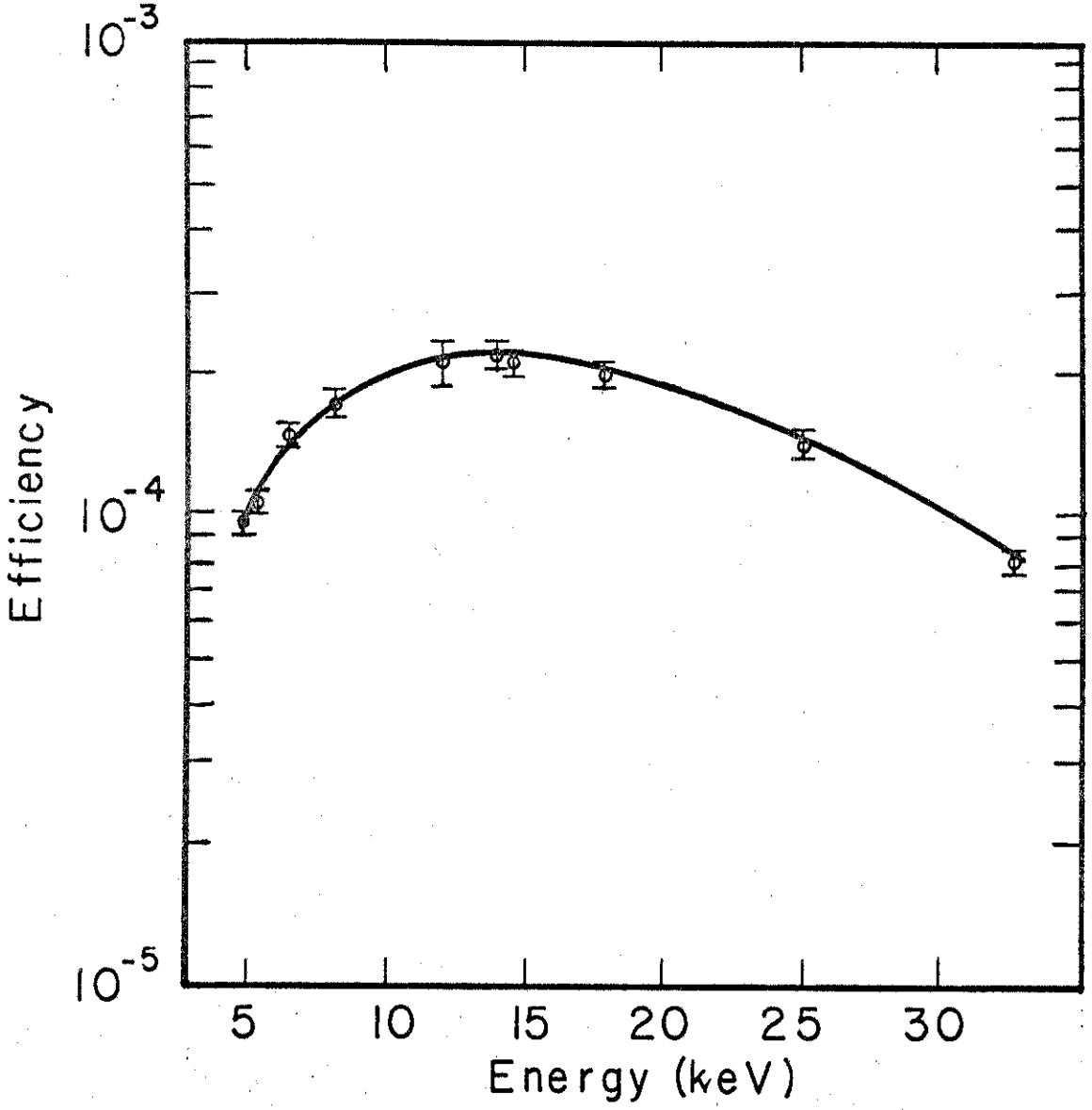

Fig. 5--Detector-System Efficiency

TABLE II

TARGET THICKNESSES

Element	Thickness (micrograms/cm^2)
Fe	13.6 ± 1.1
Co	14.5 ± 1.1
Cu	48.4 ± 3.6
Zn	29.4 ± 22.6
Ga	38.0 ± 2.9
Ge	62.9 ± 4.7
As	172 ± 13.2

A typical set of spectra for Fe is shown in Figure 6. The peaks in the x-ray energy spectrum are $\overline{K}_{\alpha}$ and $\overline{K}_{\beta}$ respectively. Because the detector resolution is insufficient to separate the $K_{\alpha 1}$ and $K_{\alpha 2}$ lines or the $K_{\beta 1}$ and $K_{\beta 2}$ lines, these lines appear as $\overline{K}_{\alpha}$ and $\overline{K}_{\beta}$ groups respectively. The peak to background ratio is approximately 300:1. The charged particle back scattering spectrum shows the carbon peak from the backing, the thick target yield from the Faraday cup and the Fe peak which is well separated from the other components of the spectrum.

Data was recorded in a Nuclear Data 2200 analyzer system and transferred to 7 track magnetic tape for analysis. The count rate in the Si(Li) detector was monitored and maintained at less than 3000 cps to facilitate spectrum stripping by computer techniques. Peak drift and resolution broadening caused by high count rates did present some problems.

The x-ray spectra were analyzed by a version of the computer code SAMPO.[41] A Gaussian with exponential tails is fitted to the peak. The peak area is calculated and an appropriate background is subtracted. This gives the number of x-rays detected during the experiment. The charged particle data was analyzed by summing the counts in the back scattered peak and subtracting a linear background.

Data reproducibility was checked by making ten runs at each energy and checking data fluctuation. The reproducibility was found to be within statistical uncertainity which was

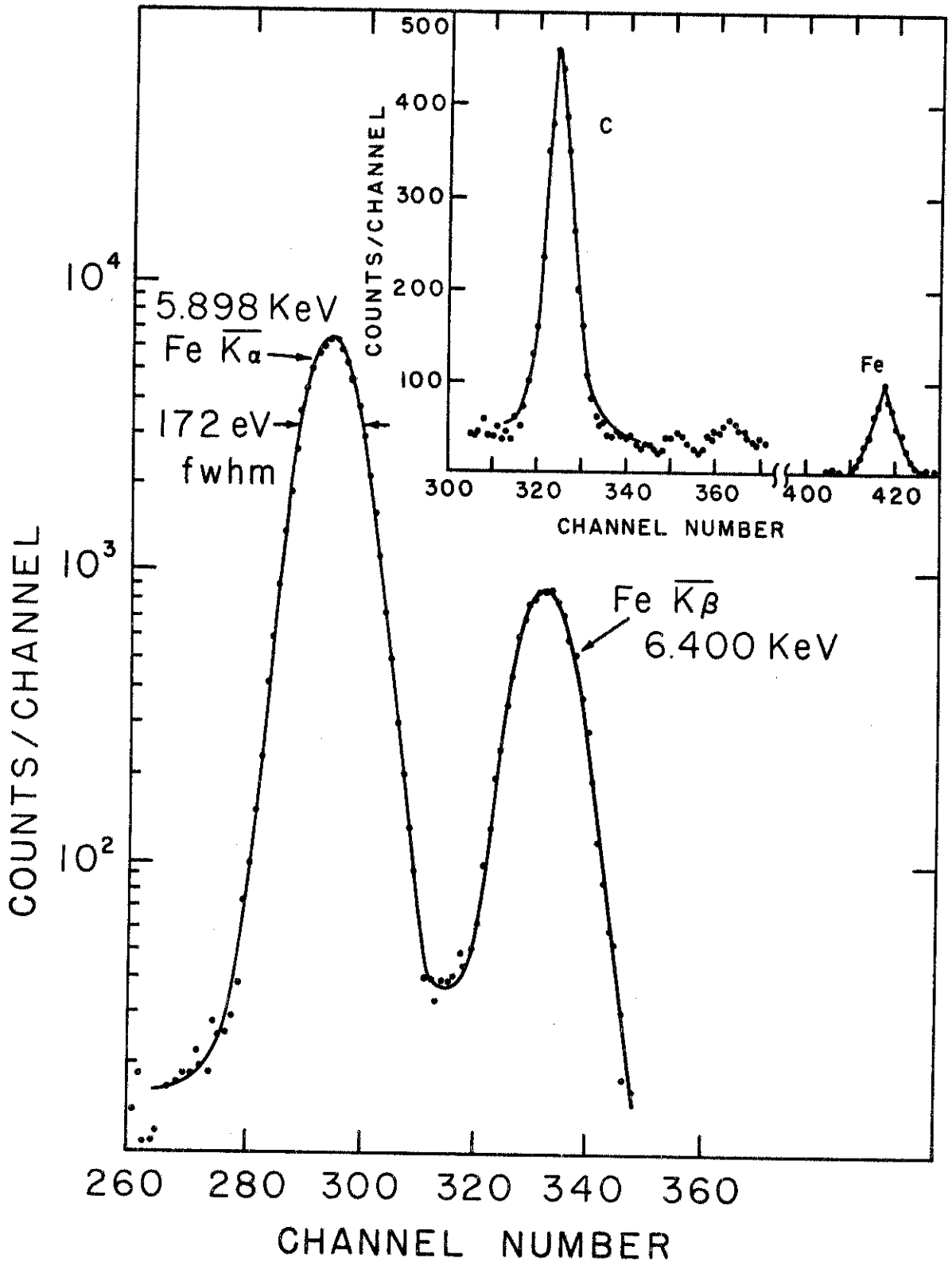

Fig. 6--Typical X-Ray and Charged Particle Spectra for Fe

typically less than one per cent. The day to day reproducibility was checked by running the same experiment on several different days and found to be within statistical uncertainity also. The reproducibility of the x-ray detector geometry was also checked using a standard source. After removing and replacing of the x-ray detector, the geometry could be reproduced to within two per cent.

Problems encountered because of boil off of target material or non-uniform targets can be minimized by using two independent analyzer systems to take simultaneous x-ray and charged particle spectra. Fluctuations in the count rate will be registered by both systems simultaneously so both spectra contain the same characteristics and no correction is needed to the data. When simultaneous spectra were taken the pulse pile-up rejector and dead time correction were disconnected from the x-ray system. This was necessary because the integrator cannot be made simultaneously compatable with both systems. Individual dead times were noted for each system and corrections were made to the data. When no target problems were encountered energy dependence of cross sections was determined by normalizing the characteristic x-ray intensity to the integrated beam and comparing intensities to the intensity at E_p = 1.5 MeV where the absolute cross section measurement was made.

An investigation of the literature reveals most measurements of ionization cross sections (σ_I) or x-ray production

cross sections (σ_x) have been made using thick targets. When thick targets are used the x-ray production cross section is given by the following expression[12]

$$\sigma_x = \frac{1}{n} \frac{dN}{dE} S(E) + \frac{1}{n} \mu N(E) \qquad (1)$$

where n is the number of atoms/gram, dN/dE is the slope of the thick target yield function in x-rays/proton/keV, S(E) is the stopping power in keV cm^2/gram, μ is the mass absorption coefficient of the target material for its own characteristic x-rays, and N(E) is the number of x-rays produced/proton. Uncertainties in experiments done with thick targets can be large because of the difficulty in evaluating the slope of the thick target yield function and the lack of reliable values of the stopping power, S(E).

Thick target problems can be reduced or eliminated by the use of thin transmission style targets. The energy lost by a 1 MeV proton in traversing a 100 microgram/cm^2 target of Fe is less than 3 per cent and self-absorption of characteristic radiation is less than 1 per cent. Evaluation of the cross section from the data is simplified because no thick target corrections have to be made.

When a proton beam is incident upon a foil target the number of x-rays emitted (N) is given by

$$N = N_T \sigma_x N_P$$

where N_T is the number of target atoms/cm^2 and N_P is the number of protons incident upon the target. The number of

x-rays detected (N_x) is given by

$$N_x = \varepsilon N$$

where ε is the efficiency of the detection system. Combining these equations gives the x-ray production cross section as

$$\sigma_x = \frac{N_x}{N_p} \frac{1}{N_T} \frac{1}{\varepsilon} .$$

The number of target atoms/cm^2 can be determined using back scattering techniques. A particle detector is placed at a known angle. By counting the number of protons scattered into the detector and making use of the expression for the differential Rutherford scattering cross section ($d\sigma/d\Omega$), N_T is given by the expression

$$N_c = N_T \frac{d\sigma}{d\Omega} N_p \Omega$$

where Ω is the solid angle the detector subtends with respect to the target.

The x-ray production and ionization cross sections are related by

$$\sigma_x = \sigma_I \omega$$

where ω is the fluorescence yield coefficient for the shell ionized. The values for ω_K, the K-shell fluorescence yield coefficient, used in this work were taken from the literature.[42]

The assumption made in this work is that the valid fluorescence yield is the fluorescence yield for the atom with one

K-shell electron removed, i. e. $\omega_K \simeq \omega_{Ko}$ where ω_{Ko} is the fluorescence coefficient for the single hole configuration $(1S)^1(2S)^2(2P)^6$. Calculations by Bhalla and Hein[43] have shown this assumption valid for proton energies less than 2 MeV. Richard et al.[44] have shown that for 800 keV protons on Ti the multi-hole configurations account for less than 10 per cent of the x-ray intensity.

The expression for determining the ionization cross section from the data is then given by

$$\sigma_I = \frac{1}{\omega_K} \frac{\Omega}{\varepsilon} \frac{N_x}{N_c} \frac{N_{Px}}{N_{Pc}} \frac{d\sigma}{d\Omega} \qquad (2)$$

where N_{Px} and N_{Pc} are the number of protons incident on the target during the acquisition of the x-ray and charged particle spectra respectively. This equation assumes the scattering of the incident protons is totally Rutherford. The energy dependence of the charged particle data was checked for agreement with the E^{-2} dependence of the Rutherford cross section. This agreement was found to be within statistical uncertainty. The scattering was found to be Rutherford in agreement with the work by Golovnya et al.[45] The following expression was used to calculate the differential Rutherford scattering cross section for proton scattered at 168 deg.,

$$\frac{d\sigma}{d\Omega} = 1.327 \times 10^{-27} \frac{Z^2}{E^2} \ (cm^2),$$

where E is the energy of the incident proton and Z is the atomic number of the target atom.

The standard deviation of each cross section was calculated using standard error analysis techniques. The deviations of the experimental terms in equation 2 were calculated and the deviations of the terms taken from the literature were those deviations quoted in the literature. The major contributions to the deviations of the cross section were from the deviation in the efficiency which was 6.2 per cent and the deviation in the fluorescence coefficient which was typically 3 to 5 per cent. The deviations in the cross section values are 8 to 10 per cent.

CHAPTER IV

DISCUSSION OF RESULTS

The cross sections measured in this work are listed in Table III. Comparisons are made to the data of Messelt,[11] of Ferree,[46] and of Lui[47] for the elements Fe, Co, and Cu. This work and the thin target data of Ferree and Lui generally agree to within 20 per cent. Comparisons are also made in this table to the predictions of the BEA, PWBA and corrected PWBA.

This work shows that for protons in the energy range 0.5 to 2.0 MeV incident on the elements Cu through As the BEA and the PWBA with binding energy corrections give nearly equivalent predictions to the measured values for the K-shell ionization cross sections. The BEA and the corrected PWBA give equivalent predictions for Fe and Co in the proton energy range 0.5 to 1.5 MeV. From 1.5 to 2.0 MeV the BEA predictions are in better agreement with the measured values than are the predictions of the corrected PWBA. In all cases the BEA and corrected PWBA fit the data better than the uncorrected PWBA which always gives predictions greater than the measured values.

Comparison between the data from this work and the three theoretical predictions is made in Figure 7. All data and

TABLE III

X-RAY AND IONIZATION CROSS SECTIONS FOR PROTON BOMBARDMENT

Element	Energy (MeV)	Cross Sections (barns)					
		σ_X this work	σ_I this work	σ_I Previous work	σ_I PWBA	σ_I PWBA with Corrections	σ_I BEA
Fe	2.0	76.5±6.0	242±23	244[b]	291	224	243
$\omega_K = 0.316 \pm 0.018$[a]	1.9	72.7±5.7	230±22		261	202	210
	1.8	69.2±5.4	219±21		235	181	193
	1.7	65.7±5.1	208±20		210	161	170
	1.6	56.9±4.4	180±18		186	142	148
	1.5	50.2±3.9	159±16	132[b]	164	123	127
	1.4	39.2±3.1	124±12		142	105	107
	1.3	34.4±2.7	109±11	56[c]	121	88.6	89.0
	1.2	29.6±2.3	93.7±9.2		102	73.0	73.3
	1.1	24.0±1.9	76.0±7.4	67.3[b]	83.2	58.7	58.5
	1.0	16.9±1.3	53.4±5.2		66.4	45.9	45.3
	0.9	14.2±1.1	44.9±4.4		51.2	34.0	33.9
	0.8	9.5±0.7	29.9±2.9		37.9	25.0	24.3
	0.7	7.2±0.6	22.9±2.2		26.5	17.1	16.4
	0.6	4.4±0.3	14.0±1.4		17.3	10.8	10.3
	0.5	1.4±0.1	4.3±0.4		10.2	6.1	5.8

Element	Energy (MeV)	Cross Sections (barns)					
		σ_X this work	σ_I this work	σ_I Previous work	σ_I PWBA	σ_I PWBA with Corrections	σ_I BEA
Co	2.0	59.3±4.5	173±15	212[b]	209	164	174
$\omega_K = 0.343\pm0.013$[a]	1.9	53.5±4.0	156±13		189	147	155
	1.8	46.0±3.5	134±11		170	132	137
	1.7	44.2±3.3	129±11		152	116	120
	1.6	39.1±3.0	114±10		134	102	104
	1.5	33.4±2.5	97.3±8.3	115[b]	118	88.0	89.1
	1.4	27.9±2.1	81.3±6.9		101	74.9	75.1
	1.3	24.7±1.9	72.0±6.1		86.0	62.6	62.1
	1.2	19.9±1.5	58.1±4.9		71.6	51.3	50.4
	1.1	16.5±1.2	48.0±4.1		58.3	41.1	40.0
	1.0	12.7±1.0	37.1±3.1	29.8[b]	46.2	31.9	30.9
	0.9	9.5±0.7	27.6±2.3		35.3	24.0	23.1
	0.8	6.4±0.7	18.7±1.6		25.9	17.2	16.5
	0.7	4.2±0.3	12.2±1.0		18.0	11.6	11.2
	0.6	2.7±0.2	7.8±0.7		11.5	7.1	7.1
	0.5	1.6±0.1	4.6±0.4		6.6	3.9	3.9
Cu	2.0	39.2±2.9	94.1±7.8	109[d]	119	92.5	90.7
$\omega_K = 0.343\pm0.013$[a]	1.9	35.9±2.7	86.2±7.2		108	83.4	80.3
	1.8	32.2±2.4	77.1±6.4		94.8	72.6	70.5

Element	Energy (MeV)	Cross Sections (barns)					
		σ_X this work	σ_I this work	σ_I Previous work	σ_I PWBA	σ_I PWBA with Corrections	σ_I BEA
Cu (cont.)	1.7	26.8±2.0	64.2±5.3		82.0	62.4	61.3
	1.6	23.4±1.7	56.2±4.7		70.8	53.4	52.7
	1.5	19.8±1.5	47.5±3.9	44.6[d]	61.0	45.5	44.7
	1.4	16.3±1.2	39.1±3.3		52.1	38.4	37.4
	1.3	13.4±1.0	32.1±2.7		43.9	31.9	30.8
	1.2	10.7±0.8	25.6±2.1		36.3	26.0	24.8
	1.1	8.0±0.6	19.2±1.6		29.2	20.6	19.5
	1.0	6.0±0.4	14.4±1.2		22.8	15.8	14.9
	0.9	4.1±0.3	9.9±0.8		17.9	11.6	10.9
	0.8	2.8±0.2	6.6±0.6		12.3	8.2	7.7
	0.7	1.8±0.1	4.2±0.4		8.4	5.4	5.0
	0.6	1.0±0.1	2.4±0.2		5.3	3.3	3.0
	0.5	0.5±0.1	1.2±0.1		3.0	1.8	1.6
Zn	2.0	31.9±2.5	70.9±6.9		84.0	65.2	65.9
$\omega_K = 0.45\pm0.025$[a]	1.9	28.7±2.3	63.8±6.2		75.8	58.4	58.3
	1.8	25.2±2.0	55.9±5.5		67.7	51.8	51.0
	1.7	22.2±1.8	49.3±4.8		59.9	45.5	44.2
	1.6	19.4±1.6	43.0±4.2		52.3	39.3	37.9
	1.5	16.6±1.3	39.0±3.6		45.0	33.5	32.0

Element	Energy (MeV)	Cross Sections (barns)					
		σ_X this work	σ_I this work	σ_I Previous work	σ_I PWBA	σ_I PWBA with Corrections	σ_I BEA
Zn (cont.)	1.4	14.0±1.1	31.0±3.0		38.2	28.0	26.6
	1.3	11.4±0.9	25.3±2.5		31.8	23.0	21.8
	1.2	9.1±0.7	20.3±2.0		26.0	18.6	17.4
	1.08	7.0±0.6	15.6±1.5		20.8	14.6	13.6
	0.97	5.3±0.4	11.7±1.2		16.1	11.1	10.4
	0.87	3.6±0.3	8.1±0.8		12.1	8.2	7.6
	0.77	2.6±0.2	5.9±0.6		8.6	5.8	5.3
	0.66	1.6±0.2	3.6±0.4		5.8	3.8	3.5
	0.56	0.5±0.1	1.1±0.1		3.6	2.3	2.1
	0.45	0.3±0.1	0.7±0.1		2.0	1.2	1.2
Ga	2.0	28.3±2.1	56.4±4.6		62.9	49.2	48.2
$\omega_K = 0.502 \pm 0.016$[a]	1.9	24.8±1.9	49.4±4.0		56.6	43.7	42.4
	1.8	21.9±1.6	43.6±3.6		50.4	38.4	37.0
	1.7	18.8±1.4	37.4±3.1		44.3	33.4	32.0
	1.6	16.1±1.2	32.0±2.6		38.5	28.7	27.3
	1.5	13.6±1.0	27.1±2.2		33.0	24.4	23.0
	1.4	11.1±0.8	22.2±1.8		27.8	20.3	19.1
	1.3	8.9±0.7	17.8±1.5		23.0	16.7	15.6
	1.2	7.6±0.6	15.1±1.2		18.7	13.3	12.5

Element	Energy (MeV)	Cross Sections (barns)					
		σ_X this work	σ_I this work	σ_I Previous work	σ_I PWBA	σ_I PWBA with Corrections	σ_I BEA
Ga (cont.)	1.1	5.3±0.4	10.6±0.9		14.8	10.5	9.7
	1.0	4.1±0.3	8.2±0.6		11.5	7.9	7.3
	0.9	2.7±0.2	5.4±0.4		8.6	5.8	5.3
	0.8	1.8±0.2	3.7±0.3		6.1	4.0	3.6
	0.7	1.1±0.1	2.2±0.2		4.1	2.6	2.4
	0.6	0.6±0.1	1.2±0.1		2.5	1.6	1.4
	0.5	0.3±0.05	0.5±0.1		1.4	0.8	0.7
Ge	2.0	18.5±1.4	36.5±2.7		47.7	36.9	35.4
$\omega_K = 0.508 \pm 0.014$[a]	1.9	16.0±1.2	32.0±2.6		42.3	33.7	31.3
	1.8	14.1±1.1	28.2±2.3		39.6	29.8	27.2
	1.7	12.2±0.9	24.4±2.0		34.4	25.7	23.4
	1.6	11.0±0.8	21.7±1.7		29.2	21.7	20.0
	1.5	8.7±0.6	17.2±1.4		24.3	18.0	16.7
	1.4	7.2±0.5	14.4±1.2		20.0	14.7	13.9
	1.3	6.0±0.5	11.9±1.0		16.4	11.9	11.2
	1.2	4.8±0.4	9.5±0.8		13.2	9.5	8.8
	1.1	3.7±0.3	7.2±0.6		10.6	7.4	6.8
	1.0	2.8±0.2	5.5±0.5		8.3	5.7	5.1
	0.9	2.0±0.15	4.0±0.3		6.3	4.3	3.7

Element	Energy (MeV)	Cross Sections (barns)					
		σ_X this work	σ_I this work	σ_I Previous work	σ_I PWBA	σ_I PWBA with Corrections	σ_I BEA
Ge (cont.)	0.8	1.4±0.1	2.8±0.2		4.6	3.0	2.5
	0.7	0.9±0.1	1.8±0.2		2.1	2.0	1.7
	0.6	0.5±0.05	1.0±0.1		1.8	1.2	1.1
	0.5	0.3±0.05	0.5±0.05		0.9	0.5	0.6
As	2.0	15.9±1.2	27.1±2.1		35.9	27.0	26.4
$\omega_K = 0.587 \pm 0.006$[a]	1.9	14.1±1.1	24.1±1.9		32.0	23.7	23.1
	1.8	12.2±1.0	20.8±1.6		28.1	20.8	20.0
	1.7	10.4±0.8	17.8±1.4		24.4	18.1	17.2
	1.6	8.8±0.7	15.0±1.2		21.0	15.6	14.5
	1.5	7.4±0.6	12.7±1.0		17.8	13.3	12.1
	1.4	6.0±0.5	10.3±0.8		14.9	11.0	10.0
	1.3	4.8±0.4	8.2±0.6		12.2	8.9	8.0
	1.2	3.8±0.3	6.5±0.5		9.9	7.1	6.4
	1.1	2.8±0.2	4.8±0.4		7.8	5.4	4.9
	0.99	2.1±0.2	3.5±0.3		6.0	4.0	3.7
	0.89	1.4±0.1	2.3±0.2		4.4	2.9	2.7
	0.78	0.9±0.1	1.6±0.1		3.1	2.0	1.9
	0.68	0.5±0.05	0.9±0.1		2.0	1.3	1.2
	0.57	0.3±0.05	0.5±0.05		1.2	0.8	0.7
	0.47	0.1±0.02	0.2±0.05		0.6	0.5	0.4

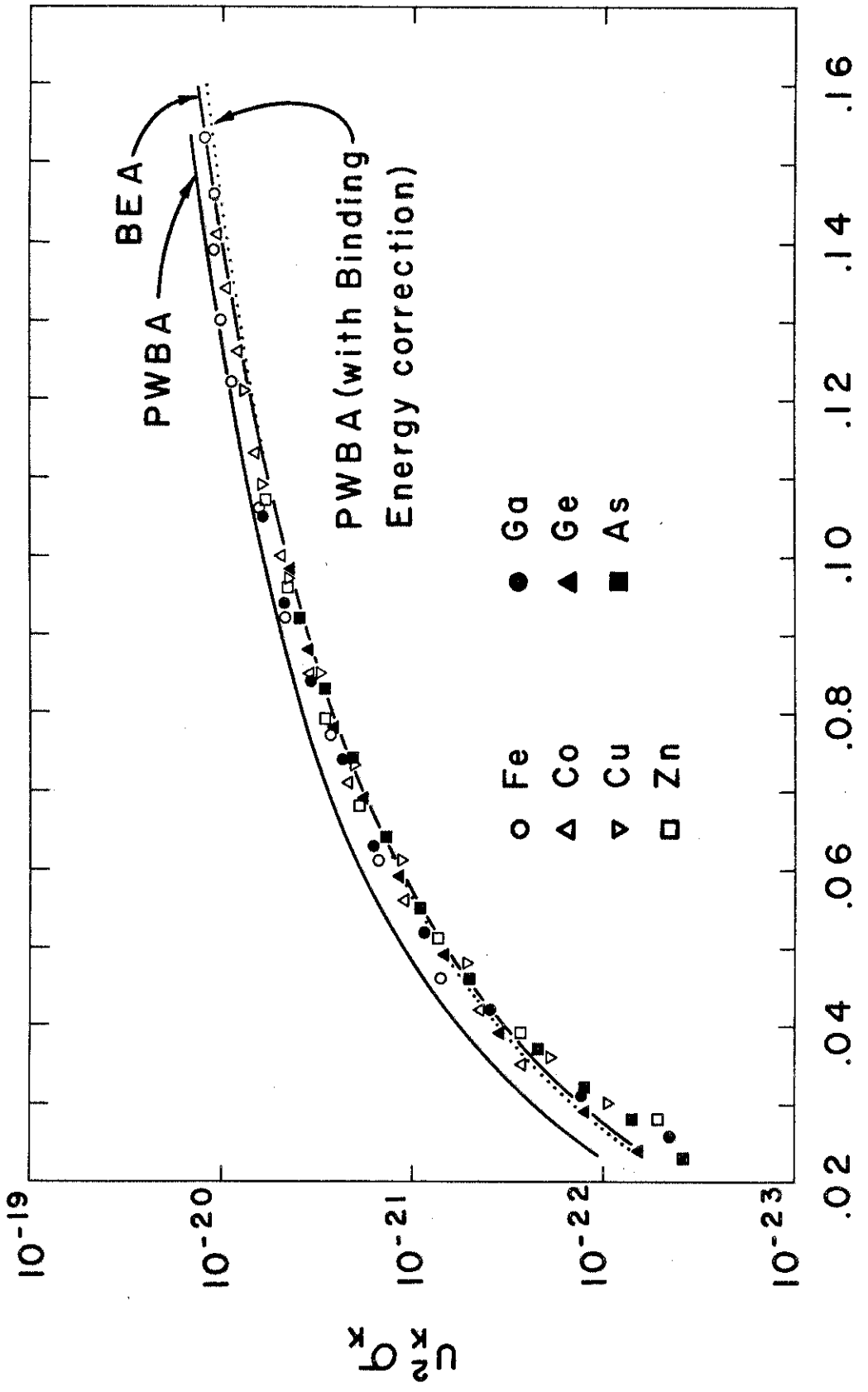

Fig. 7--Universal Cross Section Curve

theoretical predictions are plotted in terms of the units used in the BEA. The abscissa is in units of the dimensionless quantity $E/(\lambda U_K)$ where λ is the ratio of the proton mass to the electron mass, E is the energy of the incident proton and U_K is the K-shell ionization energy. The ordinate is in units of $\sigma_I U_K^2$. The use of this system of units allows all data to be plotted on one universal curve which allows the overall fit of the theory to be investigated.

The predictions of the PWBA with binding energy corrections fall below the measured values for $0.035<E/(\lambda U_K)<0.17$. This is in agreement with previous investigations by Brandt.[41] Polarization effects have not been included in the PWBA calculations. The BEA predictions fall below the measured values for $0.035<E/(\lambda U_K)<0.13$. In the range $0.13<E/(\lambda U_K)<0.17$ the measured values for Co and the BEA predictions for Fe are in agreement. The measured values and the BEA predictions are in agreement again at $E/(\lambda U_K)\simeq 0.155$. The region below $E/(\lambda U_K) = 0.035$ suggest that both the BEA and the corrected PWBA tend to overestimate the measured cross sections. In all cases the PWBA without corrections overestimates the observed K-shell ionization cross sections for the elements studied in this work.

Figure 8 shows the goodness of fit of the theory to the data as a function of $E/(\lambda U_K)$. The BEA seems to more correctly predict the energy dependence than does the corrected PWBA. The corrected PWBA underestimates the observed cross

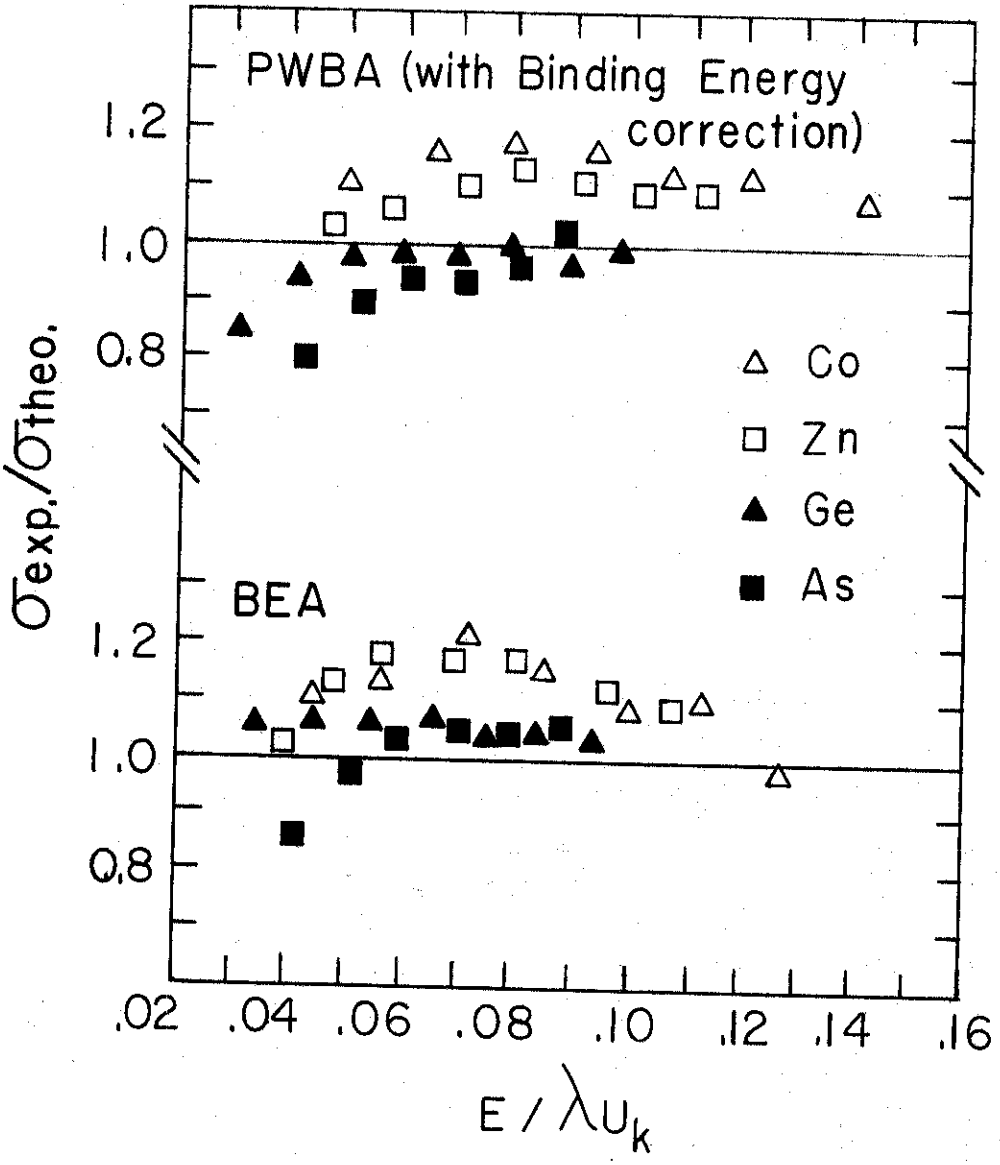

Fig. 8--Comparison of Experimental and Theoretical Cross Sections

sections at the higher values of $E/(\lambda U_K)$ and overestimates for the smaller values, whereas the BEA underestimates the observed ionization cross sections except at the lower end of values investigated.

The results of this work show the BEA and corrected PWBA give equivalent predictions for the purpose of applications of x-ray techniques. These results do suggest further work at the low energy end of the excitation curve. It is also noted that the disagreement between the data and the predictions of the BEA and corrected PWBA is increasing for decreasing Z of the target as exhibited by the Fe and Co results of this work. This suggests that further work be initiated to investigate the elements lighter than Fe in order to assess the systematics of the K-shell x-ray production processes in comparison to the theories for this proton energy range (0.5 to 2.0 MeV) and target mass range.

APPENDIX A

The BEA predicts that the theory should follow a general curve for proton bombardment of all elements. The independent variable in this theory is $E/(\lambda U_K)$. The dependent variable is $U_K^2 \sigma/Z_1^2$. These symbols have been identified in Chapter II. E and U_K must be given in keV and σ will be in cm^2.

For 2000 keV protons on zinc, $Z_1 = 1$ and $U_K = 9.66$ keV. Substituting these values into the above expression gives the independent variable as

$$E/(\lambda U_K) = 2000/(1836 \times 9.66) = 0.113.$$

Garcia[31] has published a table which gives values of $U_K^2 \sigma/Z_1^2$ for corresponding values of $E/(\lambda U_K)$. Because $E/(\lambda U_K) = 0.133$ is not given in the table, the proper value of $U_K^2 \sigma/Z_1^2$ must be extrapolated from the table which gives

$$U_K^2 \sigma = 6.15 \times 10^{-21}.$$

Solving this equation for σ gives

$$\sigma = 6.15 \times 10^{-21}/(9.66)^2 = 6.59 \times 10^{-23} cm^2.$$

Thus the BEA prediction for the cross section for ionization of the K-shell of Zn by 2 MeV protons is 65.9 barns.

APPENDIX B

The ionization cross section predicted by the PWBA is given by the expression

$$\sigma_s = 8\pi Z^2 a_o^2 Z_s^{-4} \eta_s^{-1} f_s$$

where

$$\eta_s = \frac{m_e}{m_p} \frac{E}{Z_s^2 R_\infty} .$$

The symbols used in this theory are identified in Chapter II. The factor f_s is obtained from a table published by Khandelwal *et al.*[24] by knowing the value of η_s and θ_s where

$$\theta_s = U_s s^2/(Z_s^2 R_\infty).$$

For K-shell ionization by proton impact

$$\theta_K = 73.497 U_K/(Z - 0.3)^2,$$

$$\eta_K = 0.04E/(Z - 0.3)^2$$

and

$$\sigma_K = \frac{7.038 \times 10^{-16} f_K}{(Z - 0.3)^4 \eta_K}$$

where Z is the atomic number of the target atom and E and U_K are given in keV.

The equations hold for K-shell ionization by proton impact of any atom. For 2000 keV protons on Zn

$$\eta_K = \frac{(0.04)(2000)}{(30 - 0.3)^2} = 0.091$$

and

$$\theta_K = \frac{(73.497)(9.66)}{(30 - 0.3)^2} = 0.805 \ .$$

Extrapolating the tables to give the value of f_K corresponding to the above values of η_K and θ_K gives

$$f_K = 9.58 \times 10^{-3}.$$

Substituting these values into the expression for the cross section gives.

$$\sigma_K = \frac{(7.038 \times 10^{-16})(9.58 \times 10^{-3})}{(29.7)^2(0.091)} = 8.4 \times 10^{-23} \text{cm}^2.$$

The PWBA prediction for the cross section for ionization of the K-shell of Zn by 2 MeV protons is 84.0 barns.

APPENDIX C

The change in binding energy caused by the penetration of the incident proton into the shell being ionized is given by Basbas *et al.*[34] as

$$U' = \varepsilon U$$

where

$$\varepsilon = 1 + \frac{2Z_1}{Z_K \Theta_K} g(\xi_K)$$

and $g(\xi_K)$ is given to within 1 per cent by

$$g(\xi_K) = (1 + \xi_K)^{-5}(1 + 5\xi_K + 7.14\xi_K^2 + 4.27\xi_K^3 + 0.947\xi_K^4)$$

where $\xi_K = 2\eta_K^{1/2}/\Theta_K$.

Identification of symbols is made in Chapter II.

From Appendix B,

$$\eta_K = 0.091$$

and

$$\Theta_K = 0.805$$

for 2000 keV protons incident on zinc. Substituting these values into the expression for ξ_K gives

$$\xi_K = 0.1749.$$

Substitution of ξ_K in the expression for $g(\xi_K)$ gives

$$g(\xi_K) = 0.662.$$

The expression for ε then becomes

$$\varepsilon = 1 + \frac{(2)(0.662)}{(30 - 0.3)(0.805)} = 1.055.$$

Thus the perturbed ionization energy becomes

$$U' = (1.055)(9.66) = 10.19 \text{ keV}.$$

The calculation of the cross section now proceeds the same as that for the PWBA but with U replaced by U'. Since U only appears in the Θ_K terms this amounts to replacing Θ_K with Θ_K' given by

$$\Theta_K' = \varepsilon\Theta_K.$$

For this example

$$\Theta_K' = (1.055)(0.805) = 0.849.$$

The f_K value corresponding to these η_K and Θ_K' values is

$$f_K = 7.44 \times 10^{-3}.$$

Substitution of these values into the cross section expression gives

$$\sigma_K = \frac{(7.038 \times 10^{-16})(7.44 \times 10^{-3})}{(29.7)^2(0.091)} = 6.52 \times 10^{-23} \text{cm}^2.$$

The corrected form of the PWBA predicts the cross section for ionization of the K-shell of zinc by 2 MeV protons to be 65.2 barns, as compared to the prediction of 84.0 barns by the uncorrected form of the PWBA.

APPENDIX D

The calculations preformed in computer code(SIGCAL) are done by interpolation of existing tables for both the BEA and the PWBA. Binding energy corrections are also made to the PWBA. The calculations proceed as discussed in Appendixes A-C. The interpolation is done by first calculating the energies and corresponding cross section for the exact values given in the tables which are within the energy range specified on the range card. These values are then fitted with a polynomial and the cross sections at even energies are calculated from this polynomial. For greatest accuracy specify a range larger than the actual range of interest i. e. the range printed out was 500-2000 keV but the range card specified 300-3000 keV. Both exact values given by the tables and the interpolated values are printed out. The interpolated values should be compared to the exact values before being used.

If no projectile is specified on the projectile card (i. e. no projectile card used) the program defaults to protons.

```
C       THIS PROGRAM DOES BEA AND PWBA CALCULATIONS BY MAKING USE
C       OF PUBLISHED TABLES ON EACH THEORY
C       THE RANGES OF APPLICABILITY ARE AS FOLLOWS
C        BEA-- PROTONS ONLY--ENERGY UP TO 5 MeV--TARGETS UP TO Z = 55
C        PWBA -- PROJECTILES UP TO ALPHA PARTICLES.-- ENERGY TO 5 MEV
C        TARGETS UP TO Z = 55
C
C
C*************************************************************************
C          ******   DATA CARD FORMAT   ******                             *
C          ITEM                 COLUMNS              FORMAT                *
C          CODEWORD             1-4                  A4                    *
C          LABEL                11-20                2A4,A2                *
C          WHAT(1)              21-30                F10.0                 *
C          WHAT(2)              31-40                F10.0                 *
C          WHAT(3)              41-50                F10.0                 *
C          WHAT(4)              51-60                F10.0                 *
C          WHAT(5)              61-70                F10.0                 *
C          WHAT(6)              71-80                F10.0                 *
C*************************************************************************
C
C
C*************************************************************************
C          CODEWORD             RANGE                                      *
C          LABEL                LEAVE THIS BLANK                           *
C          WHAT(1)              MIN ENERGY (KEV)                           *
C          WHAT(2)              MAX ENERGY (KEV)                           *
C          IF THIS CARD IS OMITTED THE PROGRAM DEFAULTS TO                 *
C          RMIN = 300. -- RMAX = 3000.                                     *
C*************************************************************************
C
C
C*************************************************************************
C          CODEWORD             PROJECTILE                                 *
C          LABEL                NAME OF PROJECTILE   (IE. ALPHAS)          *
C          WHAT(1)              Z OF PROJECTILE                            *
C          WHAT(2)              MASS OF PROJECTILE (IN AMU)                *
C          IF THIS CARD IS OMITTED THE PROGRAM DEFAULTS TO PROTONS         *
C*************************************************************************
C
C
C*************************************************************************
C          CODEWORD             BEA                                        *
C          LABEL                NAME OF TARGET ELEMENT                     *
C          WHAT(1)              Z OF TARGET ELEMENT                        *
C          WHAT(2)              MASS OF TARGET ELEMENT (IN AMU)            *
C*************************************************************************
C
C
C*************************************************************************
C          CODEWORD             PWBA                                       *
C          LABEL                NAME OF TARGET ELEMENT                     *
C          WHAT(1)              Z OF TARGET ELEMENT                        *
C          WHAT(2)              MASS OF TARGET ELEMENT (IN AMU)            *
C          THE PWBA WITH BINDING ENERGY CORRECTIONS IS ALSO DONE WHEN      *
C          PWBA IS CALLED.                                                 *
C*************************************************************************
C
```

```
C
C*****************************************************************
C         CODEWORD              BOTH                              *
C         LABEL                 NAME OF TARGET ELEMENT            *
C         WHAT(1)               Z OF TARGET ELEMENT               *
C         WHAT(2)               MASS OF TARGET ELEMENT (IN AMU)   *
C         THIS CODEWORD CAUSES BOTH BEA AND PWBA SECTIONS OF PROGRAM *
C         TO BE CALLED                                            *
C*****************************************************************
C
C
C*****************************************************************
C         CODEWORD              STOP                              *
C         THIS CARD TELLS THE PROGRAM TO TERMINATE                *
C*****************************************************************
C
C        FOR EXPLANATION ON THE ACURACY OF THE CALCULATIONS SEE REFERENCE
C        FROM WHICH THE DATA TABLES WERE TAKEN
C        THE ACCURACY OF THE FITTED DATA SHOULD BE CHECKED WITH THE
C         PRECEEDING TABLE BEFORE THE FITTED VALUES ARE USED
C
      DIMENSION X(10),XLABL(10),WHAT(10)
      DATA X/4HSTOP,4HBEA ,4HPWBA,4HBOTH,4HPROJ,4HRANG/
      DATA B5,B6,B7/4HPROT,4HONS ,2H  /
      COMMON A2,A3,A4,PZ,PMASS,RMIN,RMAX,U,Z,A5,A6,A7
  100 FORMAT(A4,6X,2A4,A2,6F10.0)
   20 PMASS=1.
      PZ=1.
      A5=B5
      A6=B6
      A7=B7
      RMIN=300.
      RMAX=3000.
   90 READ(5,100)(XLABL(JJ),JJ=1,4),(WHAT(JJJ),JJJ=1,3)
      IF(XLABL(1).EQ.X(1)) GO TO 1
      IF(XLABL(1).EQ.X(2)) GO TO 2
      IF(XLABL(1).EQ.X(3)) GO TO 2
      IF(XLABL(1).EQ.X(4)) GO TO 2
      IF(XLABL(1).EQ.X(6)) GO TO 6
    5 A5=XLABL(2)
      A6=XLABL(3)
      A7=XLABL(4)
      PZ=WHAT(1)
      PMASS=WHAT(2)
      GO TO 90
    6 RMIN=WHAT(1)
      RMAX=WHAT(2)
      GO TO 90
    2 A2=XLABL(2)
      A3=XLABL(3)
      A4=XLABL(4)
      Z=WHAT(1)
      U=WHAT(2)
      IF(XLABL(1).EQ.X(2).OR.XLABL(1).EQ.X(4)) CALL BEACAL
      IF(XLABL(1).EQ.X(3).OR.XLABL(1).EQ.X(4)) CALL PWBCAL
      GO TO 20
    1 STOP
      END
```

```
      SUBROUTINE BEACAL
      DIMENSION B(50),C(50),EE(50),SIGMA(50)
      DATA B/.00835,.0167,.0250,.0334,.0417,.0501,.0584,.0668,.0751,
     C.0835,.0918,.10,.109,.117,.125,.134,.142,.159,.175,.192,.200,.217,
     C.225,.250,.275,.301,.326,.351,.417,.465,.582,.699,.815,.932,1.05/
      DATA C/.000125,.00179,.00738,.0192,.0389,.0680,.107,.157,.218,
     C.289,.371,.462,.563,.672,.790,.915,1.05,1.33,1.62,1.93,2.09,2.41,
     C2.57,3.06,3.54,4.01,4.45,4.88,5.87,6.55,7.70,8.42,8.84,9.03,9.07/
      COMMON A2,A3,A4,PZ,PMASS,RMIN,RMAX,U,Z,A5,A6,A7
  200 FORMAT(10X,F11.2,4X,F15.5)
  300 FORMAT(1H1)
  400 FORMAT(10X,' BEA IONIZATION CROSS SECTION CALCULATIONS FOR',
     C/,10X,' BOMBARDMENT OF ',2A4,A2,/,10X,' WITH ',2A4,
     C//,15X,' ENERGY',8X,' CROSS SECTION')
  500 FORMAT(///,10X,' THE FOLLOWING IS A LEAST SQUARES POLYNOMIAL FIT O
     CF')
      WRITE(6,300)
      WRITE(6,400) A2,A3,A4,A5,A6
      KNT=0
      ZP=0.
      J=0
      R=1836.929*PMASS
      D=R*U
      F=1./(U*U)
      DO 10 I=1,42
      E=B(I)*D
      IF(E.LE.RMIN) GO TO 10
      IF(E.GT.RMAX) GO TO 40
      J=J+1
      EE(J)=E
      SIG=C(I)*F*PZ*PZ*(10.**4.)
      SIGMA(J)=SIG
      WRITE(6,200) E,SIG
   10 CONTINUE
   40 WRITE(6,500)
      WRITE(6,400) A2,A3,A4,A5,A6
      CALL INTERP(EE,SIGMA,J,KNT,ZP,U)
      RETURN
      END
```

```
      SUBROUTINE PWBCAL
      DIMENSION D(20,12),G(20),THT(12),EE(50),SIGMA(50),CSIGM(50),
     CT1(20),T2(20),T3(20),T4(20),T5(20),T6(20),T7(20),T8(20),T9(20),
     CT10(20)
C
      DATA T1/6.772E-08,3.336E-07,1.746E-06,1.082E-05,3.763E-05,
     C1.999E-04,6.086E-04,1.377E-03,2.597E-03,6.636E-03,1.301E-02,
     C3.902E-02,7.727E-02,1.775E-01,2.932E-01,4.126E-01,5.293E-01,
     C6.406E-01,7.453E-01,9.336E-01/
C
      DATA T2/5.455E-08,2.706E-07,1.427E-06,8.938E-06,3.136E-05,
     C1.693E-04,5.22E-04,1.193E-03,2.273E-03,5.895E-03,1.169E-02,
     C3.573E-02,7.159E-02,1.667E-01,2.775E-01,3.922E-01,5.048E-01,
     C6.123E-01,7.134E-01,8.955E-01/
C
      DATA T3/4.433E-08,2.205E-07,1.170E-06,
     C7.403E-06,2.621E-05,1.437E-04,4.488E-04,1.037E-03,1.992E-03,
     C5.241E-03,1.050E-02,3.273E-02,6.635E-02,1.567E-01,2.627E-01,
     C3.731E-01,4.818E-01,5.857E-01,6.835E-01,8.598E-01/
C
      DATA T4/3.611E-08,1.803E-07,9.634E-07,6.151E-06,2.196E-05,
     C1.222E-04,3.862E-04,9.021E-04,1.747E-03,4.662E-03,9.452E-03,
     C2.999E-02,6.153E-02,1.473E-01,2.489E-01,3.552E-01,4.601E-01,
     C5.606E-01,6.553E-01,8.262E-01/
C
      DATA T5/3.264E-08,1.634E-07,8.752E-07,5.614E-06,2.016E-05,
     C1.127E-04,3.585E-04,8.415E-04,1.637E-03,4.399E-03,8.965E-03,
     C2.872E-02,5.926E-02,1.428E-01,2.424E-01,3.467E-01,4.498E-01,
     C5.486E-01,6.419E-01,8.101E-01/
C
      DATA T6/2.954E-08,1.481E-07,7.959E-07,5.127E-06,1.845E-05,
     C1.041E-04,3.329E-04,7.852E-04,1.534E-03,4.150E-03,8.505E-03,
     C2.750E-02,5.708E-02,1.385E-01,2.360E-01,3.384E-01,4.397E-01,
     C5.370E-01,6.288E-01,7.945E-01/
C
      DATA T7/2.426E-08,1.221E-07,6.598E-07,4.286E-06,1.554E-05,
     C8.886E-05,2.873E-04,6.843E-04,1.348E-03,3.697E-03,7.657E-03,
     C2.522E-02,5.297E-02,1.304E-01,2.238E-01,3.225E-01,4.205E-01,
     C5.147E-01,6.037E-01,7.645E-01/
C
      DATA T8/2.001E-08,1.011E-07,5.438E-07,3.593E-06,1.312E-05,
     C7.599E-05,2.484E-04,5.970E-04,1.185E-03,3.295E-03,6.897E-03,
     C2.313E-02,4.917E-02,1.227E-01,2.124E-01,3.076E-01,4.024E-01,
     C4.937E-01,5.801E-01,7.362E-01/
C
      DATA T9/1.656E-08,8.397E-08,4.580E-07,3.021E-06,1.111E-05,
     C6.510E-05,2.150E-04,5.215E-04,1.004E-03,2.938E-03,6.215E-02,
     C2.123E-02,4.566E-02,1.156E-01,2.016E-01,2.935E-01,3.852E-01,
     C4.738E-01,5.577E-01,7.095E-01/
C
      DATA T10/1.376E-08,6.999E-08,3.834E-07,2.546E-06,9.427E-06,
     C5.588E-05,1.864E-04,4.560E-04,9.199E-04,2.622E-03,5.603E-03,
     C1.949E-02,4.241E-02,1.089E-01,1.915E-01,2.802E-01,3.690E-01,
     C4.550E-01,5.364E-01,6.841E-01/
C
      DATA G/0.005,0.007,0.01,0.015,0.02,0.03,0.04,0.05,0.06,0.08,0.1,
     C0.15,0.2,0.3,0.4,0.5,0.6,0.7,0.8,1./
C
```

```
      DATA THT/0.78,0.80,0.82,0.84,0.85,0.86,0.88,0.90,0.92,0.94/
      EQUIVALENCE (D(1),T1(1)),(D(21),T2(1)),(D(41),T3(1)),
     C(D(61),T4(1)),(D(81),T5(1)),(D(101),T6(1)),(D(121),T7(1)),
     C(D(141),T8(1)),(D(161),T9(1)),(D(181),T10(1))
      COMMON A2,A3,A4,PZ,PMASS,RMIN,RMAX,U,Z,A5,A6,A7
  200 FORMAT(10X,F11.2,4X,3F15.5)
  300 FORMAT(1H1)
  400 FORMAT(10X,' PWBA IONIZATION CROSS SECTION CALCULATIONS FOR',
     C/,10X,' BOMBARDMENT OF ',2A4,A2,/,10X,' WITH ',2A4,
     C//,15X,' ENERGY',8X,' CROSS SECTION')
  500 FORMAT(///,10X,' THE FOLLOWING IS A LEAST SQUARES POLYNOMIAL FIT O
     CF')
  600 FORMAT(10X,' THE CORRECTED FORM OF THE ')
  700 FORMAT(10X,' PWBA IONIZATION CROSS SECTION CALCULATIONS FOR',
     C/,10X,' BOMBARDMENT OF ',2A4,A2,/,10X,' WITH ',2A4,
     C//,15X,' ENERGY',8X,' CROSS SECTION')
  800 FORMAT(10X,' PWBA IONIZATION CROSS SECTION CALCULATIONS FOR',
     C/,10X,' BOMBARDMENT OF ',2A4,A2,/,10X,' WITH ',2A4,
     C//,15X,' ENERGY',8X,' CROSS SECTION',4X,' CHECK')
      WRITE(6,300)
      WRITE(6,700) A2,A3,A4,A5,A6
      F=1836.929*PMASS
      KNT=0
      ZP=Z-0.3
      THETA=73.497*U/(ZP*ZP)
      DO 40 J=2,12
      JM=J-1
      IF(THETA.GE.THT(JM).AND.THETA.LT.THT(J)) GO TO 70
   40 CONTINUE
   70 FACTR=(THETA-THT(JM))/(THT(J)-THT(JM))
      JJ=0
      DO 50 K=1,20
      E=G(K)*ZP*ZP*F*(0.013606)
      IF(E.LE.RMIN) GO TO 50
      IF(E.GT.RMAX) GO TO 60
      JJ=JJ+1
      EE(JJ)=E
      DP=D(K,JM)-(D(K,JM)-D(K,J))*FACTR
      SIG=7.037*DP*PZ*PZ*(10.**8.)/(ZP*ZP*ZP*ZP*G(K))
      SIGMA(JJ)=SIG
      CE=2.*(G(K)**.5)/THETA
      GG=1.+5.*CE+7.14*(CE**2.)+4.27*(CE**3.)+0.947*(CE**4.)
      GG=GG/((1.+CE)**5.)
      EPS=1.+(2.*GG/(THETA*ZP))
      CTHTA=THETA*EPS
      CHECK=G(K)/(CTHTA*CTHTA)
      DO 80 L=2,12
      LM=L-1
      IF(CTHTA.GE.THT(LM).AND.CTHTA.LT.THT(L)) GO TO 90
   80 CONTINUE
   90 CFACT=(CTHTA-THT(LM))/(THT(L)-THT(LM))
      CDP=D(K,LM)-(D(K,LM)-D(K,L))*CFACT
      CSIG=7.037*CDP*PZ*PZ*(10.**8.)/((ZP**4.)*G(K))
      CSIGM(JJ)=CSIG
      WRITE(6,200) E,SIG
   50 CONTINUE
   60 WRITE(6,500)
      WRITE(6,400) A2,A3,A4,A5,A6
```

```
CALL INTERP(EE,SIGMA,JJ,KNT,ZP,U)
WRITE(6,300)
WRITE(6,500)
WRITE(6,600)
WRITE(6,800) A2,A3,A4,A5,A6
KNT=1
CALL INTERP(EE,CSIGM,JJ,KNT,ZP,U)
RETURN
END
```

```
      SUBROUTINE INTERP(EE,SIGMA,N,KNT,ZP,U)
      DIMENSION A(21),EE(50),SIGMA(50)
  200 FORMAT(10X,F11.2,4X,F15.5)
  300 FORMAT(10X,F11.2,4X,2F15.5)
      NUM=0
      MAX=15
      RF=10**(-8.)
      CALL CRVFIT(EE,SIGMA,N,RF,AF,NUM,MAX,A)
      E=400.
      DO 10 I=1,16
      E=E+100.
      SIG=0.
      DO 20 J=1,NUM
      FJ=J-1
      SIG=SIG+A(J)*(E**FJ)
   20 CONTINUE
      IF(KNT.EQ.0) GO TO 30
      ETA=(0.04*E)/(ZP*ZP)
      THETA=(73.497*U)/(ZP*ZP)
      CE=2.*(ETA**.5)/THETA
      GG=1.+5.*CE+7.14*(CE**2.)+4.27*(CE**3.)+0.947*(CE**4.)
      GG=GG/((1.+CE)**5.)
      EPS=1.+(2.*GG/(THETA*ZP))
      CTHTA=THETA*EPS
      CHECK=ETA/(CTHTA*CTHTA)
      WRITE(6,300) E,SIG,CHECK
      GO TO 10
   30 WRITE(6,200) E,SIG
   10 CONTINUE
      RETURN
      END
```

```
      SUBROUTINE CRVFIT(X,Y,N,RF,AF,NOW,MAX,C)
C     LEAST SQUARES POLYNOMIAL FIT SUBROUTINE
      DIMENSION A(21,21),C(21),SX(43),U(500),V(21),W(500),X(500),Y(500),
     1CX(21)
C     NOW HAS THE VALUE ZERO WHEN STARTING A NEW CURVE
      IF(NOW.LE.0)GO TO 490
   40 NN=NOW+1
      DO 470 J=NN,MAX
      CX(J)=CX(J-1)/XMAX
      NOW=J
      NM=J-1
      M=J*2-1
      SY=0.
      SX(M-1)=0.
      SX(M)=0.
      DO 180 I=1,N
      XX=X(I)/XMAX
      W(I)=W(I)*XX
      SY=SY+W(I)
      SX(M-1)=SX(M-1)+U(I)
      U(I)=U(I)*XX
      SX(M)=SX(M)+U(I)
  180 U(I)=U(I)*XX
      A(J,1)=SX(J)
      A(1,J)=SX(J)/A(1,1)
      DO 270 K=2,J
      MM=K-1
      A(J,K)=SX(NM+K)
      DO 250 L=1,MM
  250 A(J,K)=A(J,K)-A(J,L)*A(L,K)
      IF(K.EQ.J)GO TO 280
  270 A(K,J)=A(J,K)/A(K,K)
  280 V(J)=SY
      DO 300 L=1,MM
  300 V(J)=V(J)-A(J,L)*V(L)
      V(J)=V(J)/A(J,J)
      C(J)=V(J)
      M=J
  330 L=M-1
      C(L)=V(L)
      DO 360 I=M,J
  360 C(L)=C(L)-A(L,I)*C(I)
      M=M-1
      IF(M.GT.1)GO TO 330
      AF=0.
      DO 397 I=1,J
  397 C(I)=C(I)*CX(I)
      DO 450 I=1,N
      PX=C(J)
      DO 440 L=1,NM
      M=J-L
  440 PX=X(I)*PX+C(M)
  450 AF=AF+(PX-Y(I))*(PX-Y(I))
      AF=AF/SX(1)
      IF(AF.LE.RF)GO TO 480
  470 CONTINUE
  480 RETURN
  490 NOW=1
```

```
      XMAX=0.
      YMAX=0.
      DO 495 I=1.N
      XMAX=AMAX1(ABS(X(I)).XMAX)
  495 YMAX=AMAX1(ABS(Y(I)).YMAX)
      CX(1)=YMAX
      SY=0.
      DO 540 I=1.N
      U(I)=X(I)/XMAX
      W(I)=Y(I)/YMAX
  540 SY=SY+W(I)
      SX(1)=N
      A(1.1)=SX(1)
      V(1)=SY/SX(1)
      C(1)=V(1)*YMAX
      AF=0.
      DO 590 I=1.N
  590 AF=AF+(Y(I)-C(1))*(Y(I)-C(1))
      AF=AF/SX(1)
      IF(MAX.NE.1)GO TO 620
      RETURN
  620 IF(AF.GT.RF)GO TO 40
      RETURN
      END
```

BEA IONIZATION CROSS SECTION CALCULATIONS FOR
BOMBARDMENT OF ZINC
WITH PROTONS

ENERGY	CROSS SECTION
443.62	0.79086
592.67	2.05753
739.96	4.16864
889.01	7.28708
1036.29	11.46644
1185.35	16.82458
1332.63	23.36153
1481.68	30.97009
1628.97	39.75745
1774.47	49.50931
1934.17	60.33273
2076.13	72.01352
2218.09	84.65877
2377.79	98.05414
2519.75	112.52104
2821.41	142.52679

THE FOLLOWING IS A LEAST SQUARES POLYNOMIAL FIT OF
BEA IONIZATION CROSS SECTION CALCULATIONS FOR
BOMBARDMENT OF ZINC
WITH PROTONS

ENERGY	CROSS SECTION
500.00	1.21328
600.00	2.11343
700.00	3.42905
800.00	5.21155
900.00	7.49617
1000.00	10.30377
1100.00	13.64110
1200.00	17.50485
1300.00	21.88354
1400.00	26.76076
1500.00	32.11658
1600.00	37.93959
1700.00	44.21909
1800.00	50.95488
1900.00	58.15141
2000.00	65.81496

PWBA IONIZATION CROSS SECTION CALCULATIONS FOR
BOMBARDMENT OF ZINC
WITH PROTONS

ENERGY	CROSS SECTION
330.69	0.51629
440.93	1.36121
661.39	4.91529
881.85	11.39808
1102.31	20.88960
1322.78	33.22687
1763.70	64.83661
2204.63	103.09491

THE FOLLOWING IS A LEAST SQUARES POLYNOMIAL FIT OF
PWBA IONIZATION CROSS SECTION CALCULATIONS FOR
BOMBARDMENT OF ZINC
WITH PROTONS

ENERGY	CROSS SECTION
500.00	2.02286
600.00	3.64365
700.00	5.84838
800.00	8.65587
900.00	12.07708
1000.00	16.11493
1100.00	20.76384
1200.00	26.00922
1300.00	31.82599
1400.00	38.17792
1500.00	45.01364
1600.00	52.26811
1700.00	59.86162
1800.00	67.71082
1900.00	75.75572
2000.00	84.02182

THE FOLLOWING IS A LEAST SQUARES POLYNOMIAL FIT OF
THE CORRECTED FORM OF THE
PWBA IONIZATION CROSS SECTION CALCULATIONS FOR
BOMBARDMENT OF ZINC
WITH PROTONS

ENERGY	CROSS SECTION	CHECK
500.00	1.22830	0.03056
600.00	2.29774	0.03678
700.00	3.79794	0.04302
800.00	5.75519	0.04929
900.00	8.19259	0.05558
1000.00	11.12976	0.06188
1100.00	14.58101	0.06820
1200.00	18.55348	0.07454
1300.00	23.04832	0.08089
1400.00	28.03127	0.08725
1500.00	33.47678	0.09363
1600.00	39.31813	0.10002
1700.00	45.47197	0.10642
1800.00	51.85033	0.11282
1900.00	58.39856	0.11924
2000.00	65.17632	0.12567

FOOTNOTES

1. J. Chadwick, Phil. Mag. 24, 594 (1912).

2. H. Franz and W. Bothe, Z. Physik 52, 466 (1928).

3. H. A. Barton, J. Franklin Inst. 209, 1 (1930).

4. C. Gerthsen and W. Reusse, Phys. Z. 34, 478 (1933).

5. M. S. Livington, F. Genevese, and E. J. Konopinski, Phys. Rev. 51, 835 (1937).

6. W. Henneberg, Z. Physik 86, 592 (1933).

7. H. W. Lewis, B. E. Simmons and E. Merzbacher, Phys. Rev. 91, 943 (1953).

8. E. M. Bernstein and H. W. Lewis, Phys. Rev. 95, 83 (1954).

9. J. M. Hanstein and S. Messelt, Nucl. Phys. 2, 526 (1956).

10. B. Singh, Phys. Rev. 107, 711 (1957).

11. S. Messelt, Nucl. Phys. 5, 435 (1958).

12. R. C. Jopson, H. Mark, and C. D. Swift, Phys. Rev. 127, 1612 (1962).

13. J. M. Khan and D. L. Potter, Phys. Rev. 133, A890 (1964).

14. J. M. Khan, D. L. Potter and R. D. Worley, Phys. Rev. 134, A316 (1964).

15. J. M. Khan, D. L. Potter and R. D. Worley, Phys. Rev. 135, A511 (1964).

16. J. M. Khan, D. L. Potter and R. D. Worley, Phys. Rev. 136, A108 (1964).

17. J. M. Khan, D. L. Potter and R. D. Worley, Phys. Rev. 139, A1735 (1965).

18. J. M. Khan, D. L. Potter and R. D. Worley, Phys. Rev. 145, 23 (1966).

19. J. M. Khan, D. L. Potter, R. D. Worley, and H. P. Smith, Phys. Rev. 148, 413 (1966).

20. J. M. Khan, D. L. Potter, R. D. Worley, and H. P. Smith, Phys. Rev. 163, 81 (1967).

21. R. R. Hart, F. W. Reuter, H. P. Smith, Jr., and J. M. Kahn, Phys. Rev. 179, 4 (1969).

22. E. Elab and M. Nakamura, Nucl. Inst. Methods 41, 161 (1966).

23. J. D. Garcia, E. Gerjuoy and J. E. Welker, Phys. Rev. 165, 66 (1967).

24. G. S. Khandelwal, B. H. Choi and E. Merzbacher, Atomic Data 1, 103 (1969).

25. J. Bang and J. M. Hansteen, Mat-Fys. Medd., 31, No. 13 (1959).

26. T. B. Johanson, R. Akselsson and S. A. E. Johanson, Nucl. Inst. Methods 84, 141 (1970),

27. J. L. Duggan, W. L. Beck, L. Albrecht, L. Munz, and J. D. Spaulding, Advances in X-ray Analysis 15, 407 (1971).

28. J. D. McCoy, J. L. Duggan, E. L. Robinson, and S. J. Cipolla, International Symposium on the Use of Nuclear Techniques in the Basic Metals Industries, Helsinki, Finlad (1972).

29. A. A. Sterk, C. L. Marks and W. P. Saylar, Advances in X-ray Analysis 10, 299 (1967).

30. E. Gerjuoy, Phys. Rev. 148, 54, (1966).

31. J. D. Garcia, Phys. Rev. A1, 280 (1970).

32. J. D. Garcia, R. J. Fortner and T. M. Kavanagh, Rev. Mod. Phys. 45, 111 (1973).

33. E. Merzbacher and H. W. Lewis, Encyclopedia of Phys. 34, 166 (1958).

34. J. C. Slater, Phys. Rev. 36, 57 (1930).

35. G. Basbas, W. Brandt and R. Laubert, Phys. Rev. A7, 983 (1973).

36. W. Brandt, R. Laubert and I. Sellin, Phys. Rev. 151, 56 (1966).

37. W. Brandt, International Conference on Inner-Shell Ionization Phenomena, Atlanta, Georgia (1972).

38. N. F. Mott, Proc. Camb. Phil. Soc. 27, 553 (1931).

39. R. S. Gehrke and R. A. Lokken, Nucl. Inst. Methods 97, 219 (1971).

40. J. S. Hansen, J. C. Mc George, D. Nix, W. D. Schmidt-Ott, I. Unus, and R. W. Fink, Nucl. Inst. Methods 106, 365 (1973).

41. J. T. Routti and S. G. Prussin, Nucl. Inst. and Methods 72, 125 (1969).

42. W. Bambynik, B. Crasemann, R. W. Fink, H. U. Freund, H. Mark, C. D. Swift, R. E. Price, and P. Venugopala Rao, Rev. Mod. Phys. 44, 716 (1972).

43. C. P. Bhalla and M. Hein, Phys. Rev. Letters 30, 39 (1973).

44. P. Richard, M. Senglaub, B. Johnson, and C. F. Moore, Appl. Phys. Letters 21, 13 (1972).

45. V. Ya Golovnya, A. P. Klyucharev, B. A. Shilyaev, and N. A. Shilyaev, Sov. J. Nucl. Phys. 4, 547 (1967).

46. D. V. Ferree, unpublished master's thesis, Univ. of Tenn. (1972).

47. Hsing Hsyang Lui, unpublished master's thesis, Tenn. Tech. Univ. (1971).

FOOTNOTES FOR TABLE III

a. W. Banbynek, B. Crasemann, R. W. Fink, H. U. Freund, H. Mark, C. D. Swift, R. E. Price and P. Venugopala Rao, Rev. Mod. Phys. 44, 716 (1972).

b. D. V. Ferree, unpublished master's thesis, University of Tennessee (1972).

c. S. Messelt, Nucl. Phys. 5, 435 (1958).

d. Hsing Hsyang Lui, unpublished master's thesis, Tennessee Technical University (1971).